Global Biogeochemical Cycles

RESEARCH ARTICLE
10.1029/2023GB007967

Characterizing the Atmospheric Mn Cycle and Its Impact on Terrestrial Biogeochemistry

Louis Lu[1,2], Longlei Li[1], Sagar Rathod[3], Peter Hess[4], Carmen Martínez[5], Nicole Fernandez[1], Christine Goodale[6], Janice Thies[5], Michelle Y. Wong[7], Maria Grazia Alaimo[8], Paulo Artaxo[9], Francisco Barraza[10], Africa Barreto[11], David Beddows[12], Shankarararman Chellam[13], Ying Chen[14], Patrick Chuang[15], David D. Cohen[16], Gaetano Dongarrà[8], Cassandra Gaston[17], Darío Gómez[18], Yasser Morera-Gómez[19], Hannele Hakola[20], Jenny Hand[21], Roy Harrison[12,22], Philip Hopke[23], Christoph Hueglin[24], Yuan-Wen Kuang[25], Katriina Kyllönen[20], Fabrice Lambert[26,27], Willy Maenhaut[28], Randall Martin[29], Adina Paytan[14], Joseph Prospero[17], Yenny González[11,30], Sergio Rodriguez[11,31], Patricia Smichowski[18], Daniela Varrica[8], Brenna Walsh[29], Crystal Weagle[29], Yi-Hua Xiao[24], and Natalie Mahowald[1]

[1]Department of Earth and Atmospheric Sciences, Cornell University, Ithaca, NY, USA, [2]Now at Nicholas School of the Environment, Duke University, Durham, NC, USA, [3]La Follette School of Public Affairs, University of Wisconsin, Madison, WI, USA, [4]Biological and Environmental Engineering, Cornell University, Ithaca, NY, USA, [5]School of Integrative Plant Sciences, Cornell University, Ithaca, NY, USA, [6]Department of Ecology and Evolutionary Biology, Cornell University, Ithaca, NY, USA, [7]Department of Ecology and Evolutionary Biology, Yale University, New Haven, CT, USA, [8]Dip. Scienze della Terra e del Mare, University of Palermo, Palermo, Italy, [9]Instituto de Fisica, Universidade de Sao Paulo, Sao Paulo, Brazil, [10]Saw Science, Invercargill, New Zealand, [11]Izana Atmospheric Research Centre AEMET, Joint Research Unit to CSIC "Climate and Composition of the Atmosphere", Santa Cruz de Tenerife, Spain, [12]School of Geography, Earth and Environmental Sciences, University of Birmingham, Birmingham, UK, [13]Department of Civil & Environmental Engineering, Texas A&M University, College Station, TX, USA, [14]Institute of Marine Sciences, University of California, Santa Cruz, CA, USA, [15]Earth & Planetary Sciences Department, University of California, Santa Cruz, CA, USA, [16]Australian Nuclear Science and Technology Organisation, Lucas Heights, NSW, Australia, [17]Rosenstiel School of Marine and Atmospheric Science, University of Miami, Miami, FL, USA, [18]Comisión Nacional de Energía Atómica, Universidad de Buenos Aires, Buenos Aires, Argentina, [19]Instituto de Biodiversidad y Medioambiente BIOMA, Universidad de Navarra, Pamplona, España, [20]Finnish Meteorological Institute, Helsinki, Finland, [21]Cooperative Institute for Research in the Atmosphere, Colorado State University, Fort Collins, CO, USA, [22]Department of Environmental Sciences, Faculty of Meteorology, Environment and Arid Land Agriculture, King Abdulaziz University, Jeddah, Saudi Arabia, [23]Department of Chemical and Biomolecular Engineering, Clarkson University, Potsdam, NY, USA, [24]Swiss Federal Laboratories for Materials Science and Technology (EMPA), Duebendorf, Switzerland, [25]Key Laboratory of Vegetation Restoration and Management of Degraded Ecosystems, South China Botanical Garden, Chinese Academy of Sciences, Guangzhou, China, [26]Geography Institute, Pontificia Universidad Católica de Chile, Santiago, Chile, [27]Center for Climate and Resilience Research, University of Chile, Santiago, Chile, [28]Department of Chemistry, Ghent University, Gent, Belgium, [29]Energy, Environmental and Chemical Engineering, Washington University, St. Louis, MO, USA, [30]CIMEL Electronique, Paris, France, [31]Instituto de Productos Naturales y Agrobiología IPNA CSIC, La Laguna, Spain

Key Points:

- We modeled the atmospheric manganese (Mn) cycle and compared our model results to existing observations that we compiled
- Human activity contributes to ~1/3 of global atmospheric Mn, shortening the surface soil Mn turnover time by 1–2 orders of magnitude
- Mn correlates with topsoil carbon (C) in temperate and (sub)tropical forests, along with N deposition and other climatic factors

Supporting Information:

Supporting Information may be found in the online version of this article.

Correspondence to:

L. Lu,
pl230@duke.edu

Citation:

Lu, L., Li, L., Rathod, S., Hess, P., Martínez, C., Fernandez, N., et al. (2024). Characterizing the atmospheric Mn cycle and its impact on terrestrial biogeochemistry. *Global Biogeochemical Cycles*, *38*, e2023GB007967. https://doi.org/10.1029/2023GB007967

Received 8 SEP 2023
Accepted 10 MAR 2024

Author Contributions:

Conceptualization: Louis Lu, Longlei Li, Sagar Rathod, Peter Hess, Carmen Martínez, Nicole Fernandez, Christine Goodale, Janice Thies, Michelle Y. Wong, Natalie Mahowald
Data curation: Maria Grazia Alaimo, Paulo Artaxo, Francisco Barraza, Africa Barreto, David Beddows, Shankarararman Chellam, Ying Chen, Patrick Chuang, David D. Cohen, Gaetano Dongarrà, Cassandra Gaston, Darío Gómez, Yasser Morera-Gómez, Hannele Hakola, Jenny Hand, Roy Harrison, Philip Hopke, Christoph Hueglin, Yuan-Wen Kuang,

Abstract The role of manganese (Mn) in ecosystem carbon (C) biogeochemical cycling is gaining increasing attention. While soil Mn is mainly derived from bedrock, atmospheric deposition could be a major source of Mn to surface soils, with implications for soil C cycling. However, quantification of the atmospheric Mn cycle, which comprises emissions from natural (desert dust, sea salts, volcanoes, primary biogenic particles, and wildfires) and anthropogenic sources (e.g., industrialization and land-use change due to agriculture), transport, and deposition, remains uncertain. Here, we use compiled emission data sets for each identified source to model and quantify the atmospheric Mn cycle by combining an atmospheric model and in situ atmospheric concentration measurements. We estimated global emissions of atmospheric Mn in aerosols (<10 μm in aerodynamic diameter) to be 1,400 Gg Mn $year^{-1}$. Approximately 31% of the emissions come from anthropogenic sources. Deposition of the anthropogenic Mn shortened Mn "pseudo" turnover times in 1-m-thick surface soils (ranging from 1,000 to over 10,000,000 years) by 1–2 orders of magnitude in industrialized regions. Such anthropogenic Mn inputs boosted the Mn-to-N ratio of the atmospheric deposition in non-desert dominated regions (between 5×10^{-5} and 0.02) across industrialized areas, but that was still lower than soil Mn-to-N ratio by 1–3 orders of magnitude. Correlation analysis revealed a negative relationship between Mn

Katriina Kyllönen, Fabrice Lambert, Willy Maenhaut, Randall Martin, Adina Paytan, Joseph Prospero, Yenny González, Sergio Rodriguez, Patricia Smichowski, Daniela Varrica, Brenna Walsh, Crystal Weagle, Yi-Hua Xiao, Natalie Mahowald
Formal analysis: Louis Lu, Longlei Li, Sagar Rathod, Natalie Mahowald
Funding acquisition: Natalie Mahowald
Investigation: Louis Lu, Sagar Rathod, Natalie Mahowald
Methodology: Louis Lu, Longlei Li, Sagar Rathod, Nicole Fernandez, Michelle Y. Wong, Natalie Mahowald
Project administration: Natalie Mahowald
Resources: Natalie Mahowald
Software: Louis Lu, Longlei Li, Sagar Rathod, Natalie Mahowald
Supervision: Natalie Mahowald
Validation: Louis Lu, Natalie Mahowald
Visualization: Louis Lu, Natalie Mahowald
Writing – original draft: Louis Lu, Natalie Mahowald
Writing – review & editing: Louis Lu, Longlei Li, Sagar Rathod, Peter Hess, Carmen Martínez, Nicole Fernandez, Christine Goodale, Janice Thies, Michelle Y. Wong, Maria Grazia Alaimo, Paulo Artaxo, Francisco Barraza, Africa Barreto, David Beddows, Shankarararman Chellam, Ying Chen, Patrick Chuang, David D. Cohen, Gaetano Dongarrà, Cassandra Gaston, Darío Gómez, Yasser Morera-Gómez, Hannele Hakola, Jenny Hand, Roy Harrison, Philip Hopke, Christoph Hueglin, Yuan-Wen Kuang, Katriina Kyllönen, Fabrice Lambert, Willy Maenhaut, Randall Martin, Adina Paytan, Joseph Prospero, Yenny González, Sergio Rodriguez, Patricia Smichowski, Daniela Varrica, Brenna Walsh, Crystal Weagle, Yi-Hua Xiao, Natalie Mahowald

deposition and topsoil C density across temperate and (sub)tropical forests, consisting with atmospheric Mn deposition enhancing carbon respiration as seen in in situ biogeochemical studies.

1. Introduction

The contribution of manganese (Mn) as an essential micronutrient to biogeochemical carbon (C) cycling has been increasingly recognized in both terrestrial and marine environments. Though often in trace amount, Mn has the potential to act as the driving factor for biogeochemical cycling when it becomes limiting in various ecosystems (Ahlgren et al., 2014; Browning et al., 2021; J. A. M. Moore et al., 2021; O. W. Moore et al., 2023; Whalen et al., 2018). Despite its importance to advancing the understanding of ecosystem functioning, little effort has been made to constrain and quantify different components of the global Mn biogeochemical cycle, let alone the atmospheric Mn cycle. Atmospheric deposition has been identified to serve as a major source of trace metal(loid)s to soils on land (He & Walling, 1997; Herndon et al., 2011; Kaste et al., 2003; Puchelt et al., 1993; Wang et al., 2022) as well as surface water in ocean (Mahowald et al., 2018). We thus focused on delineating the atmospheric component of the global Mn biogeochemical cycle using observation-model combined approaches and thereafter presented a case study of its application to terrestrial ecosystems.

1.1. Atmospheric Mn Cycle

Metals are present in the atmosphere mainly in the form of aerosols (Mahowald et al., 2018). There are a variety of natural sources of Mn, such as desert dust (the single dominant source), sea salts, volcanoes, wildfires, and primary biogenic particles (PBPs) (Nriagu, 1989; Pacyna & Pacyna, 2001). In addition to natural sources of atmospheric Mn deposition, humans can perturb the global atmospheric Mn cycle by significantly altering desert dust cycling and adding anthropogenic emission sources such as combustion (Mahowald et al., 2018). Anthropogenic aerosols have the potential to induce a more rapid impact on ecosystems compared to natural aerosols because of their higher solubility owing to their smaller particle size, higher carbon content, chemical and surface associations, and reactions that occur during the process of combustion (Desboeufs et al., 2005; Jang et al., 2007; Sedwick et al., 2007; Voutsa & Samara, 2002).

While global budgets for many metals have been estimated previously, their spatial distribution is more unknown. Nriagu (1989) made the first attempt to estimate Mn emissions to the atmosphere. Nriagu (1989) and Pacyna and Pacyna (2001) identified desert dust as the single dominant source and estimated the contribution of anthropogenic sources to be approximately 11%. Mahowald et al. (2018) estimated that anthropogenic emissions represent ∼1% of the total aerosol Mn sources. Uncertainties are high due to the lack of observational data, and so far, there have been no detailed spatially explicit studies of the atmospheric Mn cycle. Therefore, a better estimation of the Mn source budget (both natural and anthropogenic) along with its spatial distribution is necessary for understanding the global Mn cycle and its influence on terrestrial ecosystems.

In this study, we conducted the first 3-d modeling of the emission, atmospheric transport, and deposition of atmospheric Mn from multiple sources including natural and anthropogenic dust, sea salts, volcanoes, wildfires, and PBPs. We compiled emission data sets for each source and soil Mn concentration measurements for the emission modeling and model calibration, respectively. We synthesized observational and modeling evidence to characterize the spatial distribution of atmospheric Mn and to assess the anthropogenic perturbation to it in both $PM_{2.5}$ and PM_{10} size fractions (atmospheric particulate matter, PM, <2.5 and 10 μm in aerodynamic diameter, respectively), which were used as common measures for aerosols in the atmosphere and included in the model (Mahowald et al., 2014; Ryder et al., 2019).

1.2. Relevance to Terrestrial Ecosystems

Mn has been identified to be closely related to forest soil C turnover because of its role in regulating soil organic matter (SOM) decomposition by enhancing the activity of lignin-decay enzymes (mainly Mn peroxidase, MnP) and hence the oxidative decomposition of lignin (Berg et al., 2007; Hofrichter, 2002). Mn limitation and the associated fungal community change from nitrogen (N) deposition have been proposed as an explanation for the suppressing effect of long-term atmospheric N deposition on SOM decomposition (J. A. M. Moore et al., 2021;

Whalen et al., 2018). Thus, higher Mn availability from anthropogenic activity could minimize the soil carbon accumulation observed under N deposition.

Studies have assessed the relationship between Mn availability and soil C turnover rates using various indicators including Mn concentration in litter, rate or extent of decomposition of litter (Berg, 2000; Berg et al., 2007, 2010; Davey et al., 2007; Trum et al., 2015), soil Mn and total C concentrations (Stendahl et al., 2017), MnP enzymatic activity, and fungal community structures (Kranabetter et al., 2021; J. A. M. Moore et al., 2021; Whalen et al., 2018). However, no previous study has examined the impact of atmospheric Mn deposition (despite its potential to be the major source of Mn addition in surficial layers) on soil C turnover, nor has such a relationship been quantified on a global scale.

Therefore, we made a first attempt to tease out the potential relationship between Mn deposition and SOM in global forest ecosystems based on modeled Mn deposition, testing relationships between Mn availability and broad scale patterns. To understand the importance of atmospheric deposition as a flux in the Mn cycle and as a source of Mn addition to soils in terrestrial ecosystems, we interpreted soil Mn "pseudo" turnover times and Mn-to-N ratios in deposition as well as the relationship between Mn deposition and C density in topsoil.

2. Materials and Methods

2.1. Soil Mn Observations and Interpolation

Two of the outlined major emission sources, desert and agricultural dust, are directly related to Mn concentration in surficial soil layers. On average, the upper continental crust, in part based on loess analyses, contains 0.1% manganese oxide by weight (Rudnick & Gao, 2003), which is equivalent to 775 mg kg^{-1} of Mn. However, soil Mn composition can deviate from this value depending on the in-situ weathering status of the regolith and external inputs of Mn (Brantley & White, 2009). Considering this spatial heterogeneity, an inverse distance weighted (IDW) interpolation approach was taken based on 2,068 field observations compiled from 94 studies found using the Thomson Web of Science Core Collection on 20 March 2022 and the soil characterization database provided in National Cooperative Soil Survey, NCSS (Figure 1a; Text S1 in Supporting Information S1). The observations suggested a mean topsoil Mn concentration of 681 mg kg^{-1}, which is slightly smaller than, but close enough to the value derived from the averaged upper crust; therefore, a base case was set up assuming a constant soil Mn concentration of 775 mg kg^{-1} and used for comparison with the interpolated soil map in model analysis.

The constructed soil map from linear IDW interpolation was a fairly good representation of observations ($r = 0.66$; Figure 1b) given the model grid resolution and the fact that many observational sites clustered in a single grid. There were many more observations in developed countries (especially North America and Europe) in the Northern Hemisphere mid-latitudes than the higher latitudes and the tropics, where the distance to the nearest observation could be large (Figure S1a in Supporting Information S1). To partly cover the uncertainties arising from the sparseness of observational sites, an uncertainty value that equals one standard deviation (after removing outliers $>Q3 + 1.5 * \text{IQR}$ or $<Q1 - 1.5 * \text{IQR}$), 393 mg kg^{-1}, was assigned to each grid in the interpolated soil map and used along with the constant Mn base case in later sensitivity tests for "pseudo" turnover times computation. A cross validation was conducted for the interpolation to further evaluate its robustness (Figure S1b in Supporting Information S1).

2.2. Atmospheric Modeling

We simulated global atmospheric Mn emissions, transport, and deposition using the Community Atmosphere Model, version 6 (CAM6), the atmospheric component of the Community Earth System Model (version 2; CESM2) developed at the National Center for Atmospheric Research (Hurrell et al., 2013; Liu et al., 2011), with the four-mode (Aitken, accumulation, coarse, and primary) modal aerosol model (Liu et al., 2016). Three out of the four modes contain dust aerosols which are modeled as eight different types of dust mineral components (Hamilton et al., 2019; Li et al., 2021, 2022; Liu et al., 2011; Scanza et al., 2015). Model simulations were conducted for 4 years, with the last 3 years (2013–2015) used for analysis (Computational and Information Systems Laboratory, 2019). We nudged the model toward MERRA2 meteorology fields (Gelaro et al., 2017).

The model simulates three-dimensional transport and wet and dry deposition for gases and particles which are internally/externally mixed within/between the modes. The dry deposition parameterization follows Petroff and Zhang (2010) as previously implemented in CAM6 (Li et al., 2022; see descriptions therein for the wet deposition

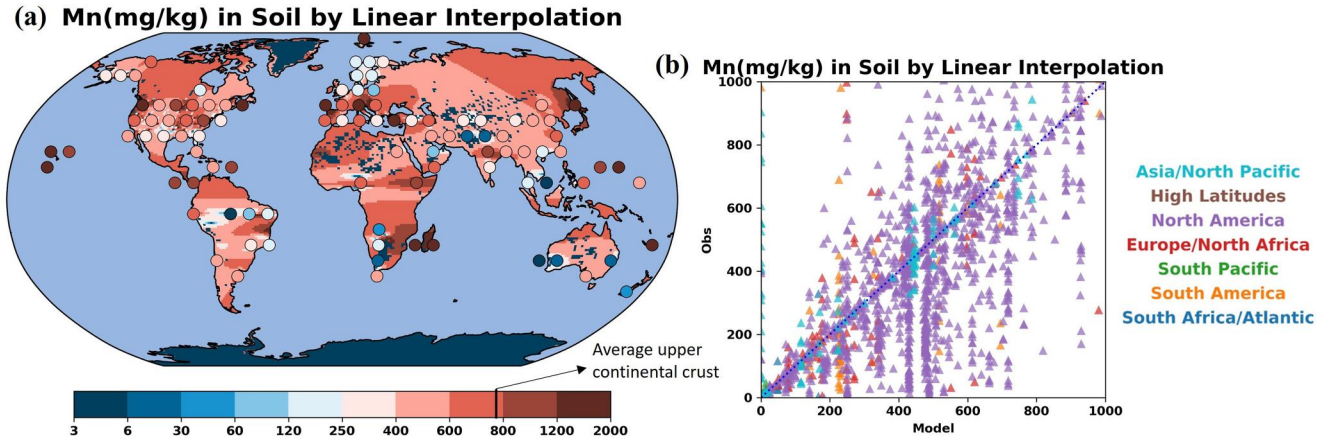

Figure 1. (a) Map of estimated global soil Mn concentration constructed from linear interpolation. The base map is compared to 2,068 individual observational points (mg kg^{-1} Mn in surface soils), which are spatially averaged and plotted as circles filled with colors corresponding to their Mn concentration (Abanda et al., 2011; Alfaro et al., 2015; Alongi et al., 2004; Andruszczak, 1975; Asawalam & Johnson, 2007; Becquer et al., 2010; Beygi & Jalali, 2018; Bibak et al., 1994; Boente et al., 2017; Bradford et al., 1996; Buccolieri et al., 2010; Burt et al., 2011; Cabrera et al., 1999; Cancela et al., 2002; Cassol et al., 2020; J. S. Chen et al., 1991; M. Chen et al., 1999, 2000; da Silva Costa et al., 2017; da Silva et al., 2015; Dantu, 2010a, 2010b; Darwish & Poellmann, 2015; de Souza et al., 2015; do Nascimento et al., 2018; Dolan et al., 1990; Fernandes et al., 2018; Foulds, 1993; Franklin et al., 2003; Ghaemi et al., 2015; Haynes & Swift, 1991; Hsu et al., 2016; Hua et al., 2013; Ikem et al., 2008; Imran et al., 2010; Iñigo et al., 2011; Ivezic et al., 2011; Jahiruddin et al., 2000; Joshi et al., 2017; Kassaye et al., 2012; Kloss et al., 2014; Lavado & Porcelli, 2000; Lindell et al., 2010; Ma et al., 1997; Mashi et al., 2004; McKenzie, 1957; Michopoulos et al., 2004, 2017; Mikkonen et al., 2017; Miko et al., 2003; Morales Del Mastro et al., 2015; Nalovic & Pinta, 1969; Nanzyo et al., 2002; Natali et al., 2009; Navas & Lindhorfer, 2005; Nguyen et al., 2018; Njofang et al., 2009; Nygard et al., 2012; Papadopoulos et al., 2009; Papastergios et al., 2011; Patel et al., 2015; Paye et al., 2010; Preda & Cox, 2002; Rashed, 2010; Rekasi & Filep, 2012; Richards et al., 2012; Roca et al., 2012; Roca-Perez et al., 2004, 2010; Rusjan et al., 2006; Saglam, 2017; Sako et al., 2009; Salonen & Korkka-Niemi, 2007; Sheikh-Abdullah, 2019; Sheppard et al., 2009; Skordas et al., 2013; Smeltzer et al., 1962; Stajković-Srbinović et al., 2018; Stankovic et al., 2012; Stehouwer et al., 2010; Steinnes et al., 2000; Sterckeman et al., 2006a, 2006b; Su & Yang, 2008; Tsikritzis et al., 2002; Tume et al., 2011; Tyler, 2004; Vance & Entry, 2000; Vejnovic et al., 2018; Wen et al., 2018; Wilcke et al., 2005; Xianmo et al., 1983; Yalcin et al., 2007; C. Yang et al., 2012; S. Yang et al., 2013; Yilmaz et al., 2003; C. Yu et al., 2012; X.-Y. Zhang et al., 2009; Zorer et al., 2009). (b) Scatter plot showing how well the linearly interpolated map represents the observations ($n = 2{,}068$, $r = 0.66$). Colors indicate the locations of studies listed in the legend. Citations of each study and details on its extraction/digestion methods are included in Supporting Information S1 (Data Set S1).

scheme as well). We modified the model to allow for the advection of Mn from different sources. Both natural and anthropogenic sources were determined to possess large uncertainties in strength. We used a first estimate assuming that the full uncertainty range is one order of magnitude. Therefore, we included a range of values (typically a factor of 10) for the Mn contribution from each source (Table 1). To better fit the observational data,

Table 1
Mn Emission Factor (Composition) in Sources and Atmospheric Mn Budgets Based on Simulations From the Community Atmosphere Model (CAM) (v6)

Source	Mn composition	Composition citation	Global source Mn (Gg $year^{-1}$) [ranges] (% fine)	Global source Mn (Gg $year^{-1}$) from reference
Desert dust	0.1–5,479 mg kg^{-1}	This study	950 [480–4,800] (1.7)	42–400[a] 900[b]
Agricultural dust	0.1–5,479 mg kg^{-1}	This study	370 [190–1,900] (1.7)	
Sea-salt aerosols	95 μg kg^{-1}	Nriagu (1989)	0.26 [0.13–1.3] (3.3)	0.02–1.7[a]
Volcanoes	12E−4 Mn/S	Nriagu (1989)	3.9 [2.0–20] (47)	4.2–80[b]
Primary biogenic particles	60 mg kg^{-1}	Nriagu (1989)	2.0 [1.0–10] (2.3)	4–50[a]
Wildfires	Fine: 0.23 mg g^{-1} Coarse: 10.58 mg g^{-1}	This study	43 [21–210] (94)	1.2–45[a]
Industrial dust	0.01–0.05 Mn/Fe	Rathod et al. (2020)	69 [35–350] (54)	10[a]

Note. Desert and agricultural dust Mn budget values were obtained from the dust model simulations which used as input the Mn composition of soils constructed using IDW interpolation (Section 2.1). Alternatively, assuming a constant soil Mn fraction (base case) yielded 1,300 Gg $year^{-1}$ and 510 Gg $year^{-1}$ (both within the uncertainty range) for desert dust and agricultural dust, respectively. [a]Nriagu (1989). [b]Mahowald et al. (2018).

we tuned the model making a particular effort to adjust anthropogenic emissions both because of their larger uncertainties compared to natural emissions and because the largest discrepancies occurred over industrialized regions (see below). The "tuning" method was based on the optimization of two parameters most related to the model performance, coefficient of determination (R^2) and root mean squared error (RMSE) and considered both natural and anthropogenic sources in both size fractions (Text S1 in Supporting Information S1). In addition, we report our best estimates and assume a large uncertainty: in most cases at least one order of magnitude because of the limited data as previous studies suggested (e.g., Mahowald et al., 2018; Nriagu, 1989).

2.2.1. Desert Dust

The desert dust sources of Mn refer to mineral particles entrained into the atmosphere by strong winds at the soil surface in arid unvegetated or loosely vegetated regions, where soils are prone to wind erosion, and play a major role in the global aerosol budget (Boucher et al., 2013; Vandenbussche et al., 2020; Zender et al., 2003). The emissions, transport, and deposition of dust aerosols, including seasonal and interannual variability, are all prognostic in the model. We applied the same dust emission scheme (Kok, Mahowald, et al., 2014; Kok, Albani, et al., 2014) as in Wong et al. (2021), and tuned the model to obtain a global mean aerosol optical depth of 0.03 (Li et al., 2022) based on observational estimates (Ridley et al., 2016). Transport and deposition of Mn were simulated separately according to the size mode (Liu et al., 2016), following treatment on dust aerosols as described in Albani et al. (2014). In addition, to improve the simulation of aerosols in the coarse and accumulation modes, we modified the model by using the geometric median diameter (GMD) as that initialized in CAM5 and geometric standard deviation as well as the edges of the predicted coarse-mode GMD following Li et al. (2022).

Because desert dust is generated from soil, we assumed that the soil Mn concentration is the same as the Mn in the dust, regardless of particle size, as we had no information on the size segregation of the soil Mn. The model simulation using the interpolated Mn soil map had Mn emissions in desert dust of 950 Gg year^{-1}, which was lower compared to 1,300 Gg year^{-1} in the base case which assumed a constant soil Mn fraction (Table 1). Both are larger than the range (42–400 Gg year^{-1}) stated in Nriagu (1989), and more similar to the value (900 Gg year^{-1}) given by Mahowald et al. (2018). Note that the amount of dust is very sensitive to the size range included in the estimates (e.g., Mahowald et al., 2014). Using the range of values from the literature, the uncertainty range of 480–4,800 Gg Mn year^{-1} was assigned.

2.2.2. Agricultural Dust

Agricultural land use and land cover change induced by human activities can boost mineral dust emissions through various mechanisms that increase soil erodibility, such as increasingly exposing soil surface and altering hydrologic cycles (Ginoux et al., 2012; Webb & Pierre, 2018). Satellite-based analysis suggests that it represents 25% of global dust emissions (Ginoux et al., 2012). To account for agricultural dust, we applied data sets of crop fraction of present agricultural land from the Coupled Model Intercomparison Project Phase 5 (CMIP5) data sets (Hurtt et al., 2011). We separately computed the crop sources of dust (identified using the above data set) and tuned these sources for each region to match those estimated from satellites, with the exception of Australia, where we assumed only 15% of the dust is anthropogenic, consistent with other studies (e.g., Bullard et al., 2008; Mahowald et al., 2009; Webb & Pierre, 2018). The discrepancy in Australia between the results of Ginoux et al. (2012) and other studies (Table S1 in Supporting Information S1) may be caused by the large drought during the time period studied by Ginoux et al. (2012). Whether agriculture has significantly altered the Mn concentration at the soil surface remains uncertain, therefore, we adopted the same interpolated soil map for calculation of Mn fraction as in the case of desert dust. This approach provides a global emissions of 370 Gg Mn year^{-1} with a range of 190–1,900 Gg Mn year^{-1} (Table 1).

2.2.3. Sea Spray

Sea-spray aerosols are produced by the bubble-bursting process typically resulting from whitecap generation under high wind conditions in the boundary layer (O'Dowd & de Leeuw, 2007). We used prognostic sea spray included in CAM6 (Liu et al., 2011) and assumed a constant concentration of 95 μg Mn kg^{-1} in sea-spray aerosols (Nriagu, 1989). Sea-spray aerosols were estimated to emit 0.26 Gg Mn year^{-1} with an uncertainty range of 0.13–1.3 Gg Mn year^{-1} (Table 1), falling within the range given by Nriagu (1989).

2.2.4. Volcanoes

Studies have shown that volcanoes can be an important contributor to trace elements in aerosols, such as Mn, through eruptive activities and degassing (Mahowald et al., 2018; Sansone et al., 2002). We assumed only non-eruptive sources for this study (Spiro et al., 1992), with a constant source across the time periods. For volcanic sources, the concentration of trace elements is commonly expressed using their ratio to sulfur (S). We adopted a mass-based ratio of 12×10^{-4} Mn/S from Nriagu (1989) and multiplied it with the concentration of sulfur given in the data set (Spiro et al., 1992) to derive Mn. We estimated non-eruptive volcanic emissions to be 3.9 Gg Mn $year^{-1}$ with a range of 2.0–20 Gg Mn $year^{-1}$, lying at the lower end of the range provided by Nriagu (1989) (Table 1).

2.2.5. Primary Biogenic Particles

PBPs are a diverse group of airborne particles such as bacteria, fungal spores, pollen, viruses and algae that are directly released from the biosphere into the atmosphere (China et al., 2020; Després et al., 2012). Like volcanoes, they are not explicitly simulated in the default CAM6 model but act as a non-negligible aerosol metal source (Mahowald et al., 2018). Following Brahney et al. (2015), we adopted parameterized PBP data that are temporally constant and based on the assumption of a leaf area index dependent source for vegetative and insect debris. We also included a pollen source based on Heald and Spracklen (2009) and a bacteria parameterization (Burrows et al., 2009). The emission, transport, and deposition of PBPs were simulated using a separate tracer. We assumed the Mn fraction to be 60 mg kg^{-1} in PBPs (Nriagu, 1989) and estimated its emission to be 2.0 Gg Mn $year^{-1}$ with a range of 1.0–10 Gg Mn $year^{-1}$ (Table 1).

2.2.6. Wildfires

Aerosols emitted from wildfires can significantly contribute to atmospheric Mn (Nriagu, 1989), especially in densely forested regions that are fire-prone (Krawchuk et al., 2009). Various emission data sets that use satellite-based remote sensing or other black carbon (BC) proxies are available for wildfires (van der Werf et al., 2004; Van Marle et al., 2017). Here, we employed the Coupled Model Intercomparison Project (CMIP6) wildfire data set as the source of BC emissions (Van Marle et al., 2017), taking advantage of its coverage of both natural fires and human influence on wildfires, including deforestation fires and control of current wildfires. To convert BC to Mn concentrations, we calculated the Mn to BC ratios in coarse (PM_{10}) and fine ($PM_{2.5}$) fractions (similar to Hamilton et al., 2022; Mahowald et al., 2005) using observational data at specific sites located in the Amazon rainforest and upper southern Africa dominated by wildfires (Maenhaut et al., 1999; Maenhaut, Fernández-Jiménez, Rajta, et al., 2000; Maenhaut, Fernández-Jiménez, et al., 2002). We derived a ratio of 10.58 mg g^{-1} for the coarse fraction and 0.23 mg g^{-1} for the fine fraction and estimated global wildfire contributions to be 43 Gg Mn $year^{-1}$ with a range of 21–210 Gg Mn $year^{-1}$ (Table 1). These values are higher than those reported in Nriagu (1989) based on more observations.

2.2.7. Industrial Emissions

Industrial emissions of Mn include anthropogenic fossil-fuel combustion, biomass burning, and related activities. Because Mn has many biogeochemical properties similar to those of Fe (Canfield et al., 2005), we assumed the co-occurrence of Mn with Fe and used an updated detailed Fe emission inventory for 2010 developed using a Speciated Pollutant Emissions Wizard (Bond et al., 2004; Rathod et al., 2020). This inventory covers Fe emission from fossil fuel burning, wood combustion, and smelting in the industrial, transport, and residential sectors globally (Alves et al., 2011; Arditsoglou et al., 2004; Block & Dams, 1976; Córdoba et al., 2012; Davison et al., 1974; de Souza et al., 2010; Dreher et al., 1997; H. K. Hansen et al., 2001; Huffman et al., 2000; Koukouzas et al., 2007; Linak et al., 2000a, 2000b; Machado et al., 2006; Mamane et al., 1986; Martinez-Tarazona et al., 1990; Meij, 1994; Querol et al., 1995; Schmidl et al., 2008; R. D. Smith et al., 1979; Steenari et al., 1999; Stegemann et al., 2000; Tsai & Tsai, 1998; Watson et al., 2001; H. Zhang et al., 2012). We then used estimates of the ratio of Mn to Fe in each type of source to obtain a new emission inventory for Mn (Table S2 in Supporting Information S1). Detailed data and citations are provided in Data Set S3. We estimated the global industrial emission to be 69 Gg Mn $year^{-1}$ and assign an uncertainty of 35–350 Gg Mn $year^{-1}$ (Table 1), assuming that the overall range will have one order of magnitude uncertainty. There is still a large uncertainty in these first estimates of Mn, and we consider elevated sources as well in later sections to better match the observational data.

2.3. Atmospheric Observations

Atmospheric observations of Mn concentrations in particulate matter (PM) were compiled and compared with the model output to assess the performance and tune the model. We compiled atmospheric Mn observational data from a variety of global data set networks and sites (Wiedinmyer et al., 2018). The available data were collected using a variety of time periods and using different chemical speciation analyses as described in detail in each study (Data Set S2). Most of the data were collected with size segregation between $PM_{2.5}$ and PM_{10} size categories (e.g., Hand et al., 2019). Some observational studies used coarse ($PM_{10–2.5}$ with aerodynamic diameter between 2.5 and 10 μm) and fine ($PM_{2.5}$) size categories instead (e.g., Maenhaut et al., 1999; Maenhaut, Fernández-Jiménez, Rajta, et al., 2000; Maenhaut, Fernández-Jiménez, et al., 2002). In this case, the two sizes were summed to compute PM_{10} for model comparison. X-ray fluorescence is the most frequently used detection method to measure Mn concentrations. The Mn quantification was unavailable at some stations if concentrations were lower than their method detection limit (MDL). In other sites Mn was measured using inductively coupled plasma mass spectrometry (ICP-MS). In total, we obtained more data points for $PM_{2.5}$ ($N = 699$) than PM_{10} ($N = 204$) because many sites focused only on $PM_{2.5}$, such as from the Interagency Monitoring of Protected Visual Environments (IMPROVE) remote/rural network in the US (Hand et al., 2017, 2019). Detailed descriptions of site and method, as well as other elemental/total Mn PM data can be found within each referenced study (Data Set S2). While there exists limited deposition elemental data, there was not enough data to warrant detailed comparisons here, and the absolute values of dry deposition were often difficult to measure (Prospero et al., 1996; Schutgens et al., 2016). We ignored particles larger than 10 μm in aerodynamic diameter here, because of the limited data, although the missed fraction of aerosols could be important for biogeochemistry in some regions (Adebiyi et al., 2023).

Hand et al. (2019) reported that collocated sites from the US Environmental Protection Agency (EPA) and IMPROVE recorded different coarse aerosol mass ($PM_{10–2.5}$), with the value at EPA sites being 10% higher than at IMPROVE sites and a 28% difference between these estimates, suggesting that different samplers could have different acuteness of size fractionation for PM_{10} and $PM_{2.5}$ (Hand et al., 2019). Overall, with a correlation coefficient of 0.9 and a slope of 0.9, the two sets of sites agreed with each other, but the difference brought by sampler biases should still be noted during later analysis and evaluation (Hand et al., 2019).

For comparison with the model, we computed annual means of atmospheric Mn concentration for each site. Particulate Mn has very low concentrations (<1 μg-m^{-3}), and therefore in many cases the data can be below the detection limit. We applied the same procedure used by Wong et al. (2021) to correct for this potential bias. If a site had more than half of its data values above the detection limit, we set the value of any samples below MDL at this site to be one-third of the MDL (shown in Data Set S2). If more than 50% of the data was below the MDL at a site, we did not include it in comparison to the model. These data were instead used to compute an upper bound based on their respective detection limits. Since many sites were close together in regions such as Europe and US, to better display the data and show the model comparison, observational data from different sites were averaged spatially within a grid cell that was two times the model resolution, or $\sim 2° \times 2°$ (Schutgens et al., 2016).

2.4. Estimation of Pseudo-Turnover Time

The importance of atmospheric Mn deposition to the upper soil Mn reservoir was evaluated by calculating the soil Mn turnover time, which is defined as the total mass of Mn in upper soil (estimated to 1 m depth) in each grid cell divided by the estimated atmospheric deposition flux from simulation. The Mn mass was calculated using the average bulk density of soil, 1.4 g cm^{-3} (C. Yu et al., 1993), and the Mn concentration, which was derived by both assuming a constant Mn concentration as in upper continental crust (base case) and applying the Mn concentration from the interpolated soil map with assigned uncertainty as upper and lower bounds for sensitivity studies. The turnover time estimated here is "pseudo-turnover time" (Wong et al., 2021) because we could not assume soil Mn to be in a steady state. The characterization of the pseudo-turnover time and comparison on a global scale allowed us to assess the ecological significance of atmospheric Mn deposition in the soil Mn reservoir in units of kiloyears (Okin et al., 2004).

2.5. Correlation Analysis and Interpretation of Ecological Relevance

Whalen et al. (2018) suggested Mn limitation as a mechanism for reduced decomposition under enhanced atmospheric N deposition; therefore, it might be helpful to consider Mn deposition together with N deposition. We

adopted a modeled annual N deposition data set (2° × 2°) (Brahney et al., 2015) and re-gridded our model output of the Mn deposition onto its resolution (2° × 2°), followed by raster calculation of the ratio of atmospheric Mn deposition to N deposition, which might provide useful insights for the relative susceptibility of soil to Mn limitation following N deposition. We compared the Mn over N ratio in deposition to the concentration ratio in soils using total N concentration data at available National Cooperative Soil Survey (NCSS) sites. The ratio was computed using both natural Mn deposition and total Mn deposition (natural + anthropogenic) to understand how and where human activities altered this ratio.

To examine how atmospheric Mn deposition potentially influences the Mn limitation that could be related to decomposition and soil C storage in forest ecosystems (Kranabetter et al., 2021; J. A. M. Moore et al., 2021; Stendahl et al., 2017; van Diepen et al., 2015; Whalen et al., 2018), we performed a spatial correlation analysis between Mn deposition and topsoil (0–5 cm) C density derived from SoilGrids 2.0, a digital soil database that includes 230,000 soil profile observations from the World Soil Information Service and applies machine learning methods (Poggio et al., 2021) to map the global distribution of soil properties at 250 m, resampled to our model resolution (1° × 1°). Mn deposition outputs derived from both the constant base case and the IDW interpolation case were compared to see how sensitive the correlation is to different approaches to calculating the Mn amounts in dust. We identified the ecosystem type at each grid cell using the plant functional types in the Community Land Model, version 5 (Lawrence et al., 2019), taking the rubric of having more than 80% of the area covered by forest biomes. Because different forest ecosystems may have distinct soil Mn status and limitation conditions (Berg et al., 2010), they were divided into three subsystems: temperate forests, subtropical and tropical forests, and boreal forests, with the correlation analysis conducted both combinedly and separately.

Because SOM decomposition has long been understood to be controlled by a combination of several different factors, Mn deposition cannot be interpreted separately from other commonly outlined predictors such as precipitation (moisture), temperature, and N deposition (Berg & Matzner, 1997; Frey et al., 2014; Hartley et al., 2021; Sierra et al., 2015; Woo & Seo, 2022; Zak et al., 2017; L. Zhang et al., 2019; F. Zhao et al., 2021). To include these potential constraints, simple and multilinear regression analyses were carried out with the addition of the three other factors: precipitation, temperature (long-term mean data from Terrestrial Air Temperature and Precipitation: 1900–2014 Gridded Monthly Time Series data provided by the NOAA PSL, Boulder, Colorado, USA, from their website at https://psl.noaa.gov), and N deposition to test the significance of Mn deposition on topsoil C density. The multilinear regression was calculated following the ordinary least squares (OLS) method.

3. Results

3.1. Mn Concentration in Atmospheric Particulate Matter (PM)

Mn in the model output was compared with the Mn concentration in atmospheric PM observation on a global scale. Here, we present three cases (Figures 2 and 3) for the simulation with dust emission schemes created by linear interpolation (Section 2.1) to better examine the model sensitivity to anthropogenic emissions. We used the bounded observational data (Section 2.3) for all comparisons and scatter plots.

The natural case (Figure 2a) was simulated without any emission from anthropogenic sources (industrial emission + agricultural dust). With only natural contributions, the model underestimated Mn concentration significantly in the PM_{10} size fraction (Figure 2b), especially over industrialized regions in Asia, Europe, and southern Africa, where the world's largest Mn mining industry is located (U.S. Geological Survey, 2022). The model also poorly simulated the relatively high Mn concentrations reported by several sites across North America. Only close to dust desert dominated regions in North Africa does the model simulate the concentrations well (Figure 2a). The spatial distribution of Mn in western North Africa agrees with the observations on the location of Mn rich dust sources (Rodríguez et al., 2020).

When anthropogenic sources were added, using the default values described in Section 2.2, the model improved the simulation in industrialized regions (Figure 3b and Figure S9 in Supporting Information S1). The value of the correlation coefficient (r) increased 3-fold with RMSE on the same level ($r = 0.089$, RMSE = 0.025 in Figure 2b; $r = 0.27$, RMSE = 0.023 in Figure 3b), suggesting that the model performance improved with the addition of anthropogenic contributions. However, Mn concentrations at the major proportion of sites were still underestimated compared with the observations. Through iterative tuning, we found that the atmospheric concentrations were best matched when we increased the anthropogenic emissions by a factor of 1.9 (Text S1 in Supporting

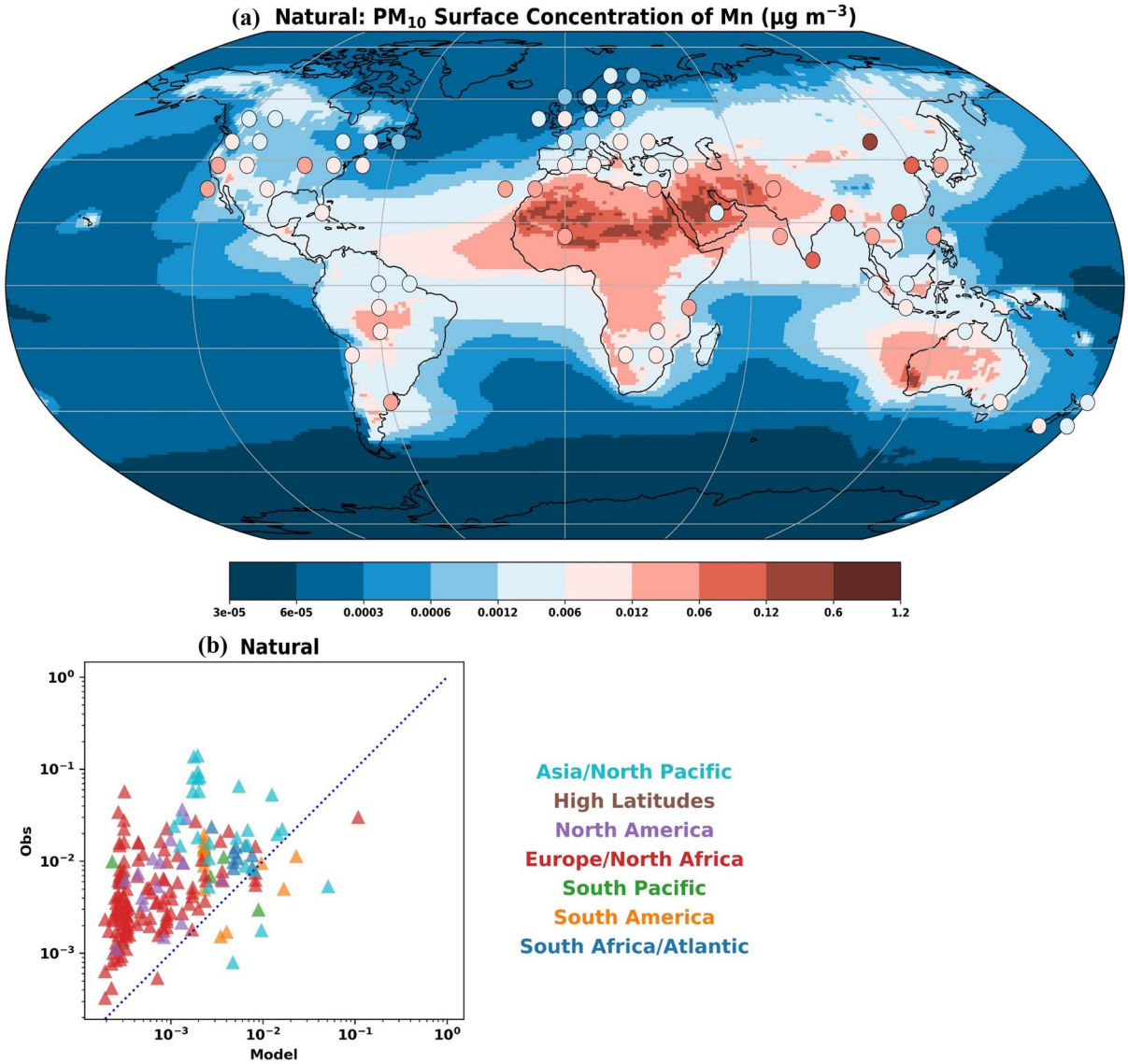

Figure 2. (a) Global distribution of the atmospheric Mn concentration at the surface in the PM_{10} size fraction from the model simulation results (contours) using only natural sources with a dust scheme constructed by linear interpolation and from bounded observations (circles). Observations were spatially averaged to a ~2° × 2° grid and compared to the Community Atmosphere Model (CAM) (v6) results. (b) Scatter plot comparison of model simulated atmospheric concentration with observations in the natural case ($n = 203$, $r = 0.089$, RMSE = 0.025). Colors of points indicate the locations of studies listed in the legend (Alastuey et al., 2016; Andreae et al., 2002; Arimoto et al., 2003, 2006; Artaxo et al., 2002; Atanacio & Cohen, 2020; Barraza et al., 2017; Bergametti et al., 1989; Bozlaker et al., 2013, 2019; Y. Chen et al., 2006; Chuang et al., 2005; Cohen et al., 2004; DFM & WSP, 2020; Dongarrà et al., 2007, 2010; European Monitoring and Evaluation Programme, 2020; Fuzzi et al., 2007; Gianini, Fischer, et al., 2012; Gianini, Gehrig, et al., 2012; Hand et al., 2017; Hsu et al., 2016; Hueglin et al., 2005; Kyllönen et al., 2020; Laing et al., 2014a, 2014b; Mackey et al., 2013; Maenhaut & Cafmeyer, 1998; Maenhaut, Cafmeyer, et al., 1997; Maenhaut, De Ridder, et al., 2002, Maenhaut, Fernández-Jiménez, et al., 2002; Maenhaut et al., 1999, 2005, 2008, 2011; Maenhaut, Fernández-Jiménez, Rajta, et al., 2000; Maenhaut, Fernández-Jiménez, Vanderzalm, et al., 2000; Maenhaut, Francois, et al., 1997; Maenhaut, Koppen, & Artaxo, 1996; Maenhaut, Salma, et al., 1996; Maenhaut, Salomonovic, et al., 1996; Malm et al., 2007; McNeill et al., 2020; Mkoma, 2008; Mkoma et al., 2009a, 2009b; Morera-Gómez et al., 2018; Nyanganyura et al., 2007; Perez et al., 2008; Putaud et al., 2004, 2010; Rodríguez et al., 2011, 2015; Salma et al., 1997; Savoie et al., 1993; Smichowski et al., 2004; Swap et al., 2002; UK Department for Environment, Food, and Rural Affairs, n.d.; Vanderzalm et al., 2003; Virkkula et al., 1999; Xiao et al., 2014).

Information S1). We defined our "best estimate" as the case with elevated anthropogenic emissions (Figures 3a and 3b) and denoted the unmodified scenario the "low anthro" case (Figure 3c). While some stations were overestimated in the best estimate case, much fewer stations were, and the data spots were distributed more uniformly along the 1:1 line of the scatter plots, with r increased to 0.36. In many of the sites, there was a mismatch between the date of the measurement and the model simulation because of limited observations.

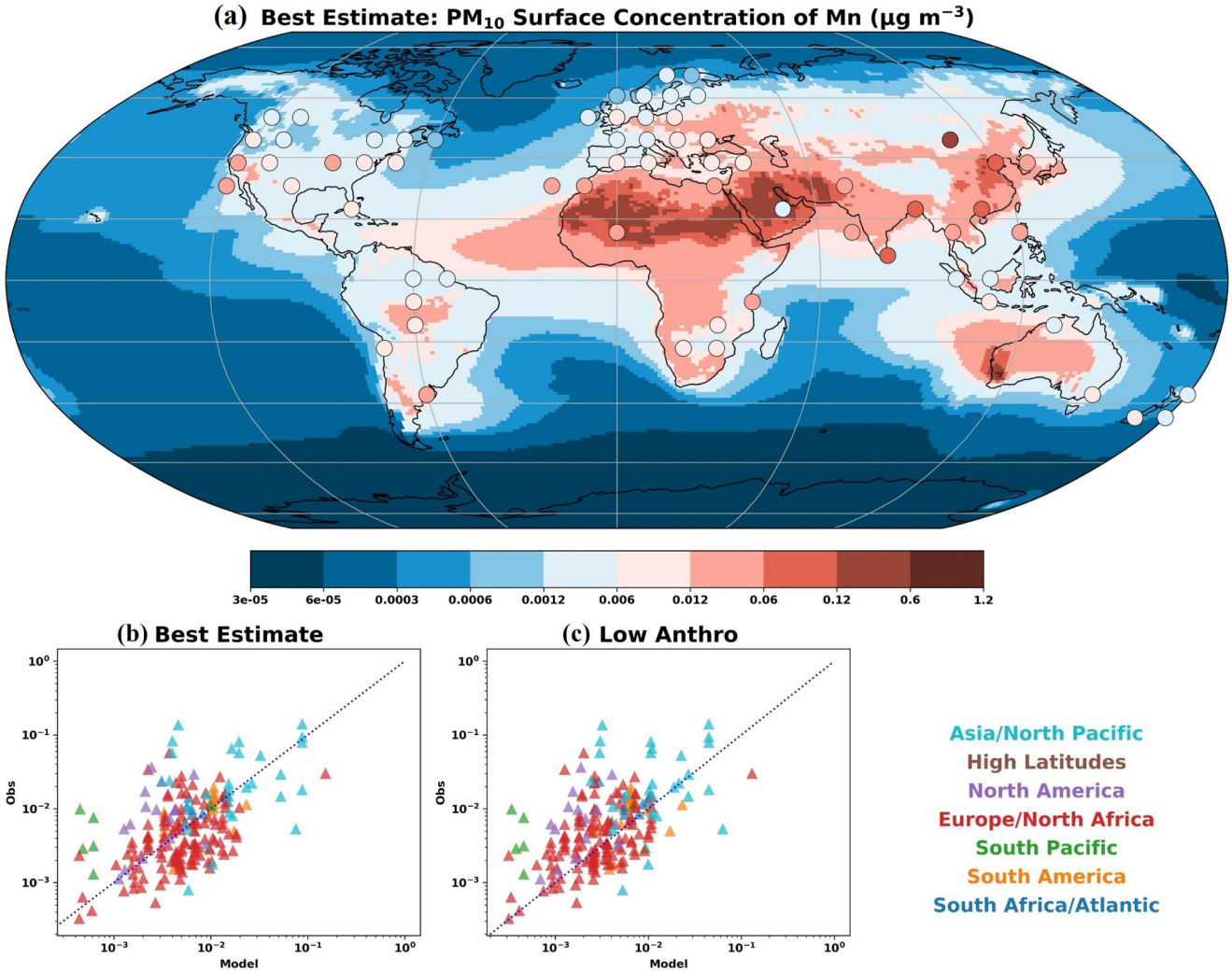

Figure 3. (a) Global distribution of the atmospheric Mn concentration at the surface in the PM_{10} size fraction from the model simulation results (contours) using the dust scheme constructed by linear interpolation in the best estimate case and from bounded observations (circles). Observations were spatially averaged to a ~2° × 2° grid and compared to the Community Atmosphere Model (CAM) (v6) results. (b) Scatter plot comparison of model simulated atmospheric concentration with observations in the best estimate case ($n = 203$, $r = 0.35$, RMSE = 0.024). Colors of points indicate the locations of studies listed in the legend. (c) Same as (b), except for the low anthropogenic model case ($n = 203$, $r = 0.27$, RMSE = 0.023).

We noticed that a few sites with high Mn concentrations across North America, including several peaks in the central United States, were still missed by the model in the best estimate case, suggesting that our estimation of anthropogenic source contributions could be lower than the actual in this region. Overall, our model agreed on the same order of magnitude of Mn concentration in atmospheric PM_{10} as the observations and had the ability to, at least, partially represent the variability in their spatial distribution.

Despite the dominance of the PM_{10} size fraction of the atmospheric Mn budget due to the coarse nature of dust (Table 1), Mn in atmospheric $PM_{2.5}$ is also important because of the high percentage of fine fraction in wildfires and industrial dust (Table 1) and the potential health risks that could be induced by inhalation of Mn in $PM_{2.5}$ in ambient air (Cavallari et al., 2008; Expósito et al., 2021). Generally, we obtained similar global distribution patterns and results of the model-observation comparison as in PM_{10}. With a more than tripled number of atmospheric Mn observations in the $PM_{2.5}$ size fraction, especially in the U.S., the model simulation better matched the observations across North America (Figure 4a). The highest observation values were reported over industrialized regions in Europe and Asia and regions affected by desert dust generated in North Africa. Our model showed elevated atmospheric Mn levels in Europe and Asia compared to the Americas. Similarly, atmospheric

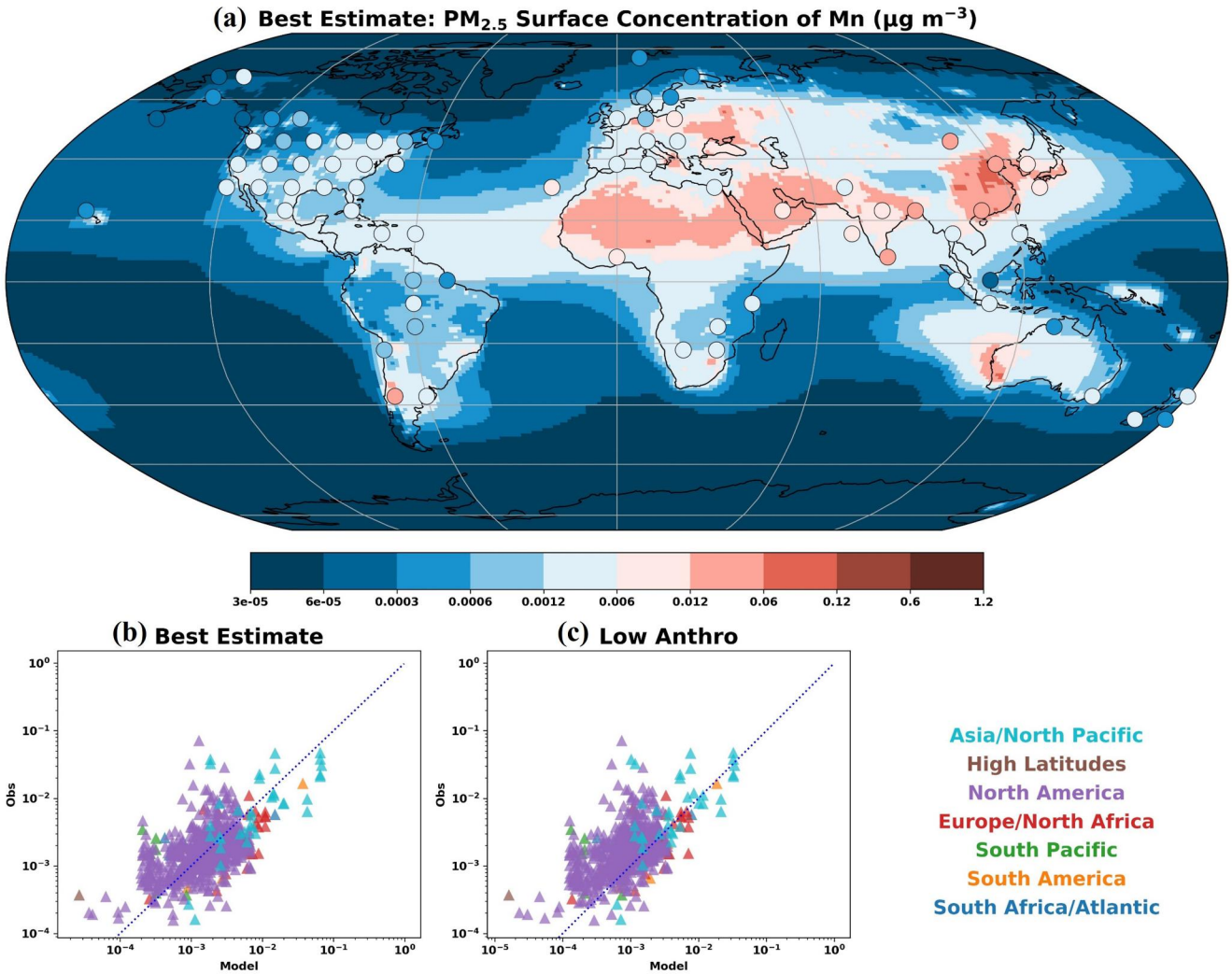

Figure 4. Same as Figure 3, but for the $PM_{2.5}$ size fraction. (a) Global distribution of the atmospheric Mn concentration at the surface from the model simulation results (contours) using the dust scheme constructed by linear interpolation in the best estimate case and from bounded observations (circles). Observations were spatially averaged to a ~2° × 2° grid and compared to the Community Atmosphere Model (CAM) (v6) results. (b) Scatter plot comparison of model simulated atmospheric concentration with observations in the best estimate case (n = 698, r = 0.53, RMSE = 0.006). Colors of points indicate the locations of studies listed in the legend. (c) Same as (b), except for the low anthropogenic model case (n = 698, r = 0.53, RMSE = 0.005).

Mn over industrialized regions was underrepresented by the model simulations in the natural case (Figure S2 in Supporting Information S1), and we derived our best estimate by tuning the level of anthropogenic emissions toward the higher end by a factor of 1.9. With the best estimate case, our model showed a moderately good representation of the observations (Figures 4b and 4c). Having more observational sites might explain the slightly better performance of the comparison in the $PM_{2.5}$ size fraction than in the PM_{10} size fraction.

We performed the same analysis using model simulations with constant soil Mn fraction (base case) and found the results changed quantitatively but not qualitatively (Figure S3 in Supporting Information S1). Surface Mn concentration was elevated in regions affected by desert and agricultural dust (e.g., larger impact of Saharan dust on the Americas and central Asia) in the base case with higher aerosol budgets in these two sources (Table 1), Both methods produced simulation results that were of similar order of magnitude as the observations, but the model built with interpolation was determined to be a better match because of its stronger correlation and smaller RMSE (Figure 3 and Figure S3 in Supporting Information S1).

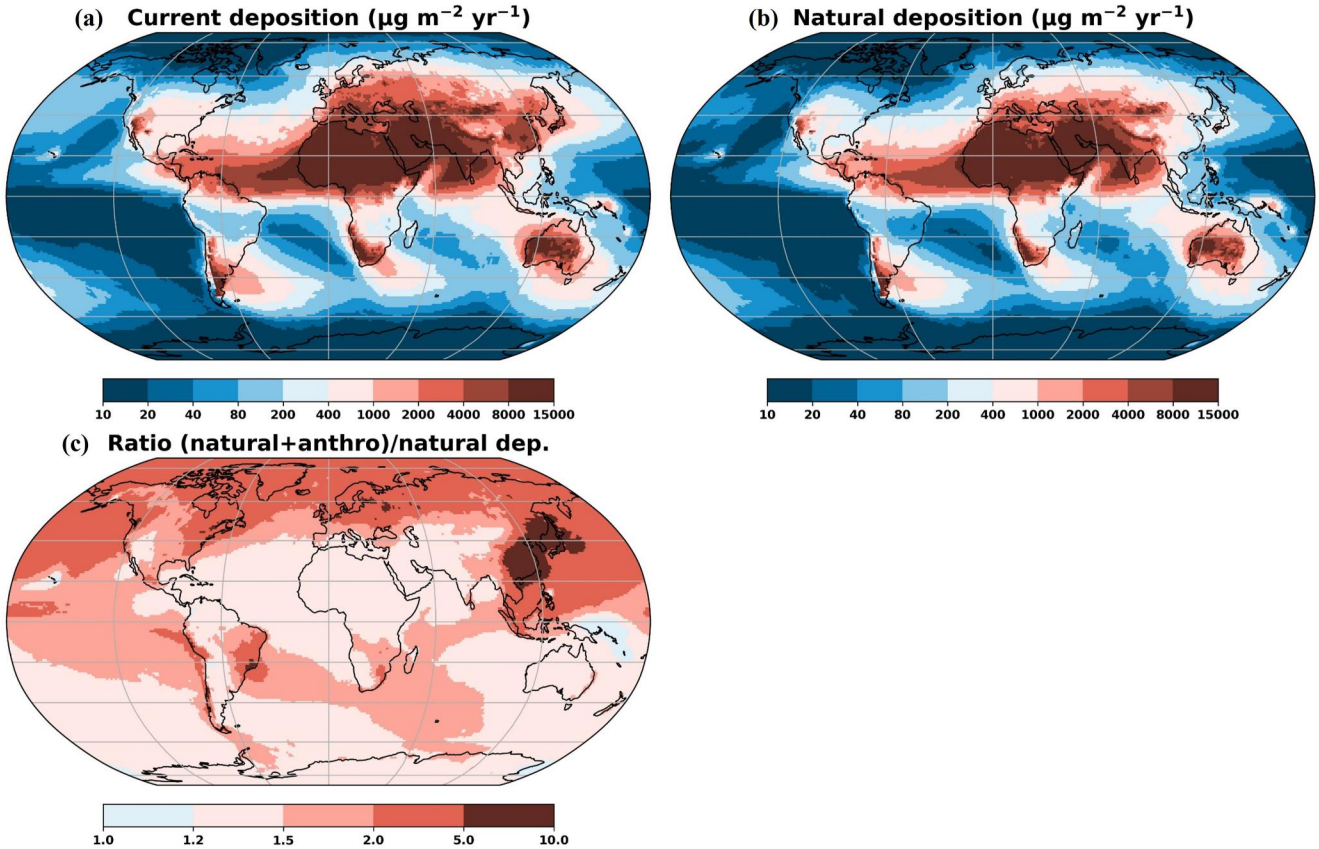

Figure 5. (a) Global pattern of the current (anthropogenic + natural sources) atmospheric Mn deposition (μg m^{-2} year^{-1}) as simulated in the Community Atmosphere Model (CAM) (v6) in the best estimate case. (b) Same as (a), except for including natural sources of emissions only. (c) Ratio of total atmospheric Mn deposition to natural deposition.

3.2. Atmospheric Mn Budget and Source Apportionment

Our model predicted the global total Mn emission to be 1,400 Gg Mn year^{-1} with a range of 730–9,700 Gg Mn year^{-1} due to the uncertainty in each source (Table 1). The estimate was similar in magnitude to the reference value of 1,000 Gg Mn year^{-1} given by Mahowald et al. (2018). The model-simulated budget for each source was within or close to the estimated range from previous studies (Mahowald et al., 2018; Nriagu, 1989). The model estimated that 1,000 Gg Mn year^{-1} was emitted from natural sources with a range of 500–5,000 Gg Mn year^{-1}, while 440 Gg Mn year^{-1} was emitted from anthropogenic sources with a range of 225–2,300 Gg Mn year^{-1} (Table 1), suggesting that 31% (best estimate, with uncertainty ranging from 4% to 82%) of the atmospheric Mn arose from anthropogenic contribution.

While anthropogenic sources contributed to a significant portion of the total atmospheric Mn budget, our model suggested that their main influence was in the Northern Hemisphere, where the ratio of total to natural deposition was significantly greater than 1 (Figure 5), and there was a high percentage of anthropogenic or industrial dust (Figures 6c and 6d), especially over industrialized regions in Asia, Europe, and the northeastern U.S. Hot spots in the Southern Hemisphere included eastern and southeastern Brazil, Peru, Chile, and southern Africa. High ratios of total to natural deposition in these regions indicated strong human perturbations (up to 10 times higher) on the Mn deposition rates (Figure 5c). Industrial emissions were responsible for major regions dominated by anthropogenic deposition, while the distribution of agricultural deposition was more dispersed, with a wider coverage of cultivated areas worldwide (Figures 6c and 6d).

Desert dust represented over 90% of all natural sources of the atmospheric Mn deposition (Table 1). It dominated deposition within major deserts in North Africa, inland Australia, and Asia as well as regions that were affected by the transportation of desert dust produced in these systems (Kellogg & Griffin, 2006). For example, the

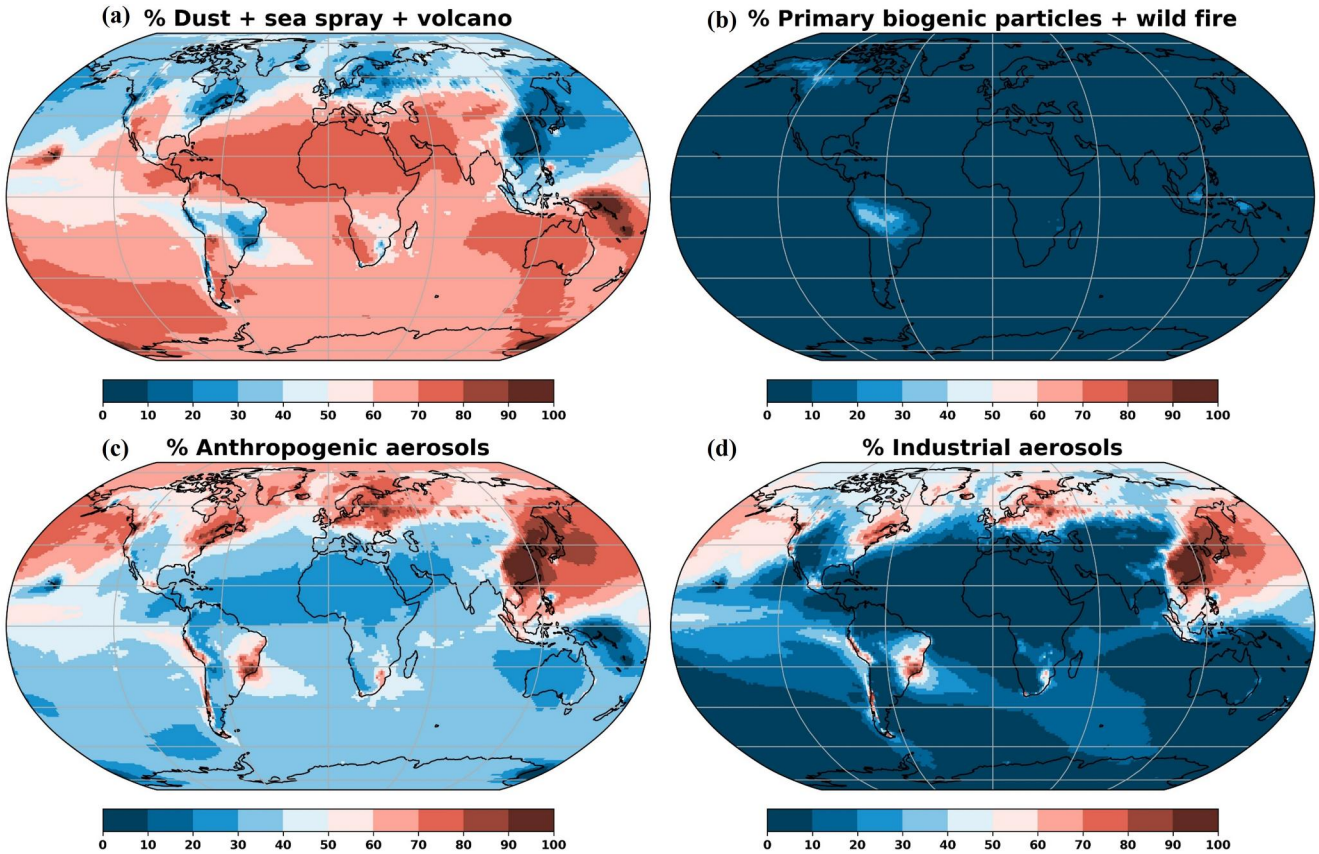

Figure 6. Source apportionment of the atmospheric Mn deposition in the best estimate case shown by percentage of different sources in the Community Atmosphere Model (CAM) (v6): (a) desert dust, sea sprays, and volcanoes, (b) primary biogenic particles and wildfires, (c) combined anthropogenic aerosols (agricultural dust + industrial emissions) and (d) industrial aerosols.

intercontinental transport of African dust to South America has been identified as an important source of new atmospheric deposition of P in the Amazon and could have a fertilization effect (Okin et al., 2004; Ridley et al., 2012; H. Yu et al., 2015). The dominance of desert dust and other natural sources (sea salts and volcanoes, which represented a very small fraction) was complementary with anthropogenic sources: desert dust dominated most of the Southern Hemisphere but became less influential at higher latitudes in the Northern Hemisphere as anthropogenic emissions concentrated there (Figure 6a).

Although wildfires have a much lower budget than desert dust, they are the second-largest natural source of atmospheric Mn (Table 1). Together with PBPs, they were major players in regions that are less affected by desert dust and anthropogenic aerosols, such as the Amazon rainforest, upper southern Africa (and Madagascar), Indonesia, northern Canada and Alaska (Figure 6b). Wildfires can displace large amounts of nutrients, including Mn, from terrestrial ecosystems (Kauffman et al., 1995; Mahowald et al., 2005) which are then replenished by transported dust and sea salts, as well as anthropogenic depositions, similar to what was reported by Wong et al. (2021) in the case of molybdenum (Mo).

3.3. Soil Mn Pseudo-Turnover Times

The pseudo-turnover time provides a metric of the ecological importance of atmospheric Mn deposition to the upper soil Mn reservoir (Okin et al., 2004). Using linear interpolation, we divided the estimated soil Mn concentration by the model simulated Mn deposition rates to compute pseudo-turnover times in upper soils (Okin et al., 2004). The estimated soil Mn pseudo-turnover time varied spatially, ranging from 1,000–10,000 years in regions dominated by desert dust to over 10,000,000 years at higher latitudes (Figure 7a). To test the sensitivity of turnover times to different dust schemes, Mn deposition simulated in the base case and the constant Mn soil map were used to compute pseudo-turnover times for comparison (Figure 7b). Again, results were qualitatively

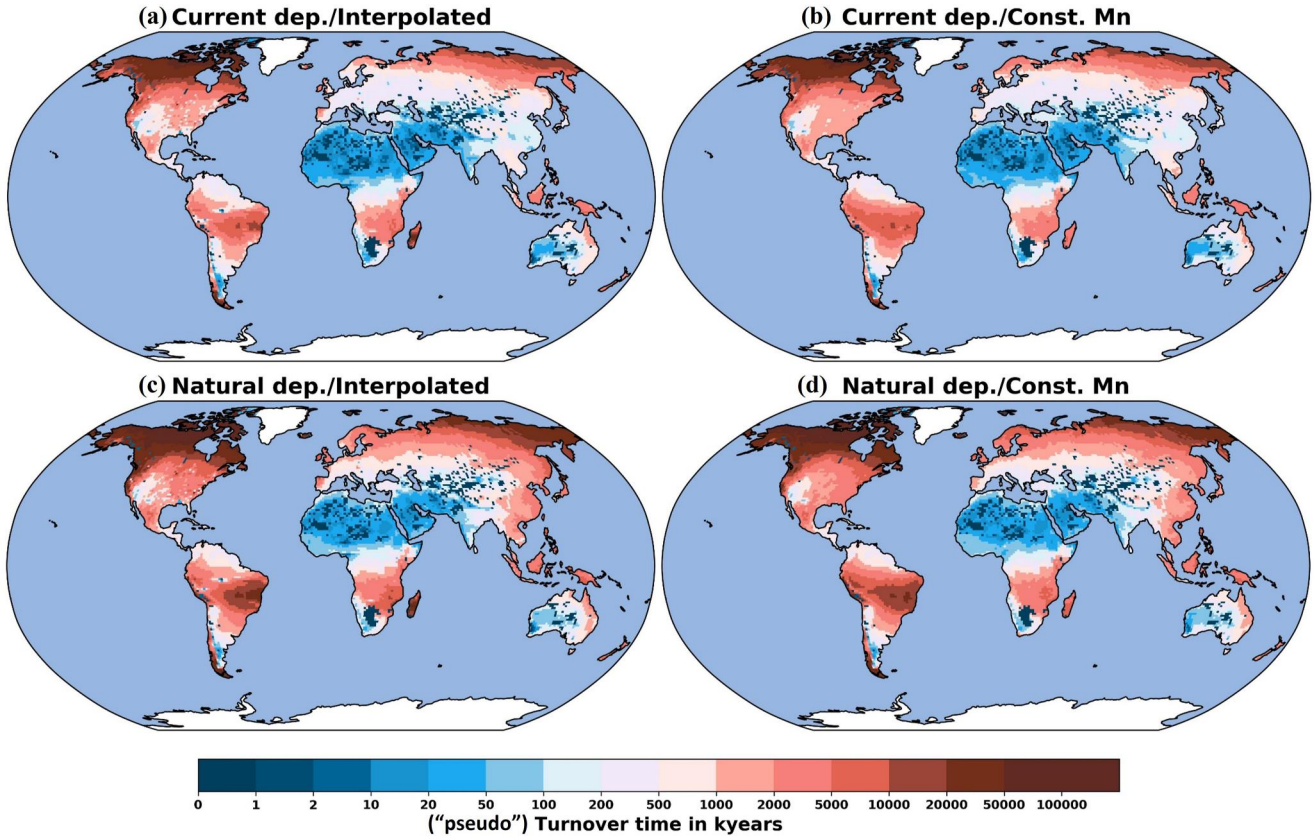

Figure 7. "Pseudo" turnover times (kiloyears) of the surface soil Mn from current (natural + anthropogenic sources) atmospheric Mn deposition as simulated in the Community Atmosphere Model (CAM) (v6) using the dust scheme constructed from (a) linear interpolation (and calculated using the linear-interpolated soil Mn map) and (b) constant soil Mn fraction (and calculated using constant soil Mn map). (c, d) Same as (a, b) except for the inclusion of only natural Mn deposition in the calculation of turnover times.

consistent despite small quantitative differences (e.g., turnover was slightly retarded in parts of the central and eastern U.S., where relatively high precipitation likely had produced a more advanced stage of weathering, deviating the soil Mn concentration from the upper crust average). We found that anthropogenic sources significantly shortened the soil Mn pseudo-turnover times in industrialized regions regardless of the interpolation method. For example, the atmospheric deposition sourced from anthropogenic emissions shortened the soil Mn pseudo-turnover time by 1–2 orders of magnitude from millions of years to as low as tens of thousands of years in eastern China and across Europe (Figures 7a, 7c and 7b, 7d). These trends indicate that human perturbation has the potential to accelerate Mn turnover in different terrestrial systems if the amount of anthropogenic activity remains at the same level or even rises in the future. The upper and lower bounds of the pseudo-turnover times were generated using those of the soil map (Figure S6 in Supporting Information S1) and could be viewed as a reference for the uncertainty, which, in general, was within 0–1 order of magnitude as the estimated value.

Compared to the Mo pseudo-turnover time of 1,000–2,000,000 years (Wong et al., 2021), the estimated range of soil Mn pseudo-turnover times is wider, and the mean turnover time is longer, which is closer to the estimated range of P pseudo-turnover time (∼104 to ∼107 years) in Okin et al. (2004). In the Amazon region, the soil Mn pseudo-turnover time ranged from hundreds of kiloyears in the northeast corner, which was subject to deposition from transported African dust, to thousands of kiloyears moving toward the central and southwestern regions. Compared to the turnover times from other studies of macronutrients, the estimated Mn pseudo-turnover time here is orders of magnitude longer than the N turnover time of 177 years globally (Rosswall, 1976) and the P turnover time of 50 years averaged across several stations in the Amazon rain forest (Mahowald et al., 2005), which was accelerated by human-induced land use change such as deforestation and biomass burning (Andela et al., 2017; M. C. Hansen et al., 2013). Overall, these comparisons illustrate the spatial variability of the soil Mn

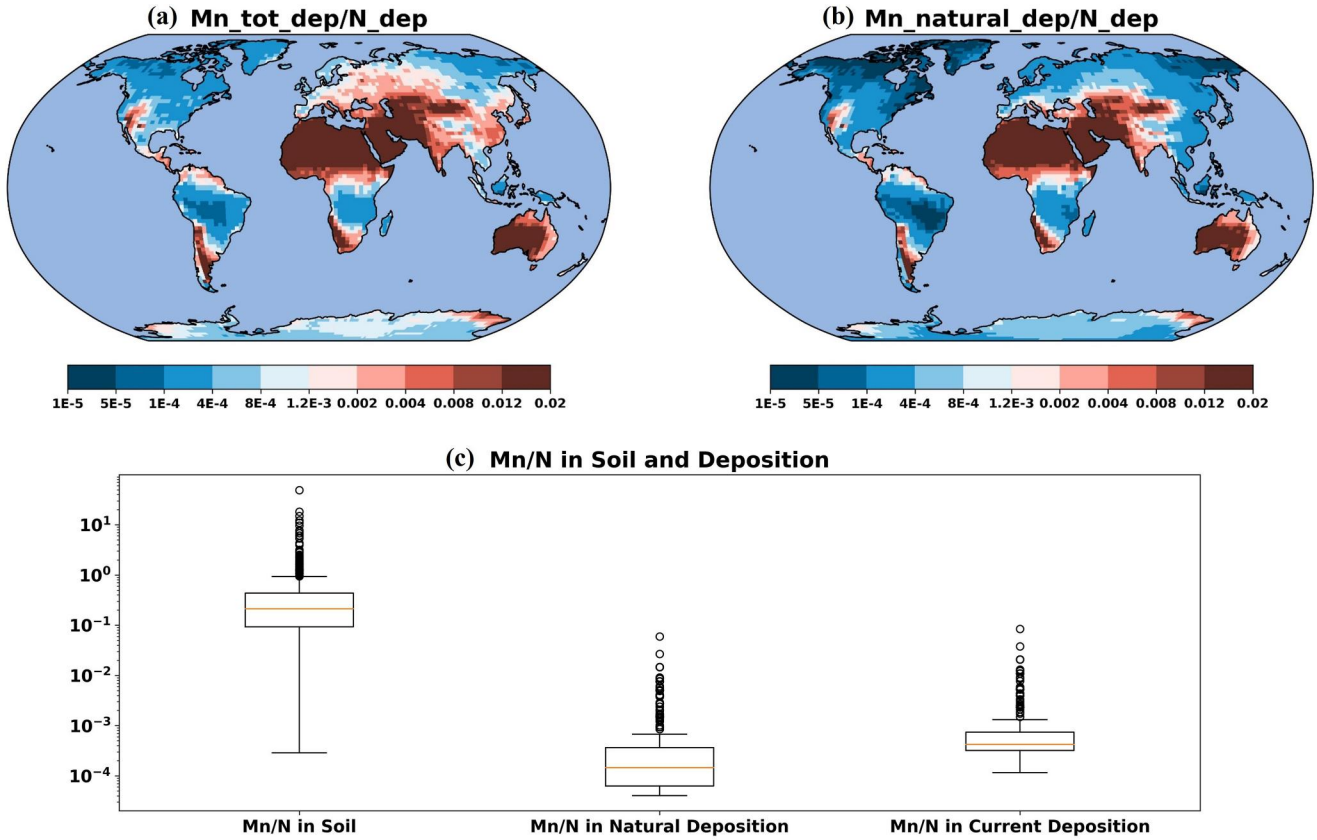

Figure 8. (a) Ratio of Mn to N in atmospheric deposition calculated using the current Mn deposition simulated in the Community Atmosphere Model (CAM) (v6) and the N deposition from Brahney et al. (2015). (b) Same as in (a), except for the inclusion of only natural Mn deposition in the calculation. (c) Box-and-whisker plot showing the Mn-to-N ratio in surficial soils at available sites and in depositions (current + natural). Circles represent outliers.

pseudo-turnover times and suggest that atmospheric deposition of Mn may play a non-negligible role in the terrestrial surface Mn cycle in many regions globally.

3.4. Linkage to N Deposition and C Storage

3.4.1. Mn to N Ratio in Deposition

In addition to characterizing the atmospheric Mn cycle itself, we tested linkages of Mn availability to surface soil C observations and projected N deposition. Mn limitation has been proposed to explain the reduced organic matter decomposition in soils under chronic atmospheric N deposition (J. A. M. Moore et al., 2021; Whalen et al., 2018), which has the potential to regulate carbon sequestration in forest soils. Here, we calculated an Mn-to-N atmospheric deposition ratio, as low Mn-to-N deposition ratios could indicate where N deposition could slow lignin decay and thus facilitate soil carbon accumulation, while high Mn-to-N ratios could indicate where surface soils may not increase in soil carbon accumulation even with high N deposition rates alone.

We found that the ratio of Mn to N in the atmospheric deposition varies globally by several orders of magnitude (Figure 8a). It could be as low as 5×10^{-5} in the northern latitudes and over 0.02 in desert dust dominated regions, where the dust composition is almost entirely of mineral nature with low N content (Davies-Barnard & Friedlingstein, 2020; Kanakidou et al., 2016). Though the variability of the ratio is less when narrowed down to forest ecosystems, it still spans orders of magnitudes. Anthropogenic emissions increased the depositional ratio of Mn-to-N in most parts of the world (even in Antarctica), with the impact in industrialized regions being the most substantial (Figure 8a). When only considering the natural sources, we estimated that the Mn-to-N ratio is moderately low in major industrialized regions including northern Europe, eastern China, and the northeastern U.S., with the U.S. having lower ratios than Asia and Europe in general (Figure 8b). Anthropogenic sources enhanced the Mn-to-N ratio in all these regions, with a stronger effect in China and Europe than in the U.S. Other

areas with low Mn-to-N ratio under current deposition were either around the equator, where much nitrogen fixation occurred in soils as the source of dust emission (Davies-Barnard & Friedlingstein, 2020), or at higher latitudes. In general, regions less affected by desert dust and anthropogenic aerosols had relatively low Mn-to-N ratios. This could be best illustrated in the Amazon Forest, where the northernmost portion influenced by African dust transportation (Ridley et al., 2012) had a much higher Mn-to-N ratio than the central part (Figures 8a and 8b).

We compared the Mn-to-N ratio in atmospheric deposition to the in-situ ratio of Mn to N concentration in surficial soils at 1,319 available sites (mainly across the U.S.). For example, Kranabetter et al. (2021) reported 541 mg kg^{-1} Mn and 0.77% total N in surficial soils in a temperate forest located on southern Vancouver Island. With the measurements in the abovementioned study, we calculated the in-situ Mn-to-N ratio in soil to be 0.067, which is over two orders of magnitude larger than the depositional Mn-to-N ratio of 0.00052 calculated using our gridded model output and the N deposition data set (extracting the value of the grid in which Vancouver Island was located). Considering all available soil observational sites that contained valid measurements of Mn and N concentrations (mainly from the NCSS data set), we obtained a median depositional Mn-to-N ratio of 0.00040 versus a median soil Mn-to-N ratio of 0.21, or typically one to three orders of magnitude lower than the soil concentration ratio (Figure 8c). Regions with disproportionally low Mn-to-N ratios in atmospheric deposition are interpreted to be the most susceptible to potential Mn limitation, such as temperate and boreal forests in north-eastern U.S., Canada, and northern Europe, in agreement with current field experimental results (Kranabetter et al., 2021; Stendahl et al., 2017; Whalen et al., 2018).

3.4.2. Correlation With Topsoil C Density

To test the significance of atmospheric Mn deposition in decreasing soil Mn limitation and thus facilitating decomposition in forest ecosystems on a global scale, we correlated our simulated atmospheric Mn deposition with the topsoil (0–5 cm) C density derived from SoilGrids 2.0 (Poggio et al., 2021) in (sub)tropical, temperate, or boreal forests. In each case, a simple linear regression between topsoil C density and each of the four factors was carried out, including Mn deposition. Our results revealed fairly good negative correlations ($r < -0.5$) between topsoil organic C density and Mn deposition in temperate ($r = -0.67$) and (sub)tropical forests ($r = -0.52$; Figure 9a). A similar negative relationship was determined between C density and N deposition in temperate forests ($r = -0.69$; Figure 9b), where a significant positive relationship was obtained in the case of precipitation ($r = 0.71$; Figure 9d). In addition, a negative correlation between C density and temperature was found only in (sub)tropical forest, though relatively weaker ($r = -0.46$; Figure 9c). When we combined the three forest ecosystems for simple regression analysis, all factors showed statistically significant correlation, with Mn deposition ($r = -0.37$, $p < 0.0001$) having the third strongest coefficient of determination (Table 2).

Using multilinear regression, we found a negative relationship between C density and Mn deposition across all forests (Table 2). Overall, the *R*-squared value of the OLS model reached 0.438, with the skew (−0.121), kurtosis (3.077), and Jarque-Bera test (1.790, $p = 0.409$) likely indicating normally distributed residuals. To check for multicollinearity, we computed a correlation matrix (Table S3 in Supporting Information S1) and found a positive correlation between Mn deposition and N deposition ($r = 0.63$, $p < 0.0001$), providing the possibility that the negative correlation between topsoil C density and Mn deposition was a "byproduct" of the positive correlation between Mn and N deposition. A calculation of variance inflation factors obtained values <2 for all individual variables (Table S3 in Supporting Information S1), suggesting that variables were only moderately correlated with each other, and multicollinearity was likely not problematic. Furthermore, we tested the correlation using normalized Mn (Mn-to-N ratio) and found it still negative and statistically significant for temperate and (sub)tropical forests (Figure S7a in Supporting Information S1). Of course, correlations can never show causality, so it is still possible that our results are spurious, but the statistical tests presented here are consistent with our hypothesis. We also conducted a correlation analysis using base case outputs under constant soil Mn assumption and found negative relationship significant regardless of the method we used to calculate Mn in dust (Figure S7b in Supporting Information S1). Therefore, it is reasonable to conclude that the Mn deposition could be a predictor of topsoil C density along with N deposition and other climatic factors in forest ecosystems (predominantly temperate and tropical). In fact, Mn addition to soils has been shown to increase C losses (e.g., CO_2 and dissolved organic carbon) during litter decomposition, suggesting increased Mn supply could result in decreased soil C storage (Jones et al., 2020; Trum et al., 2015).

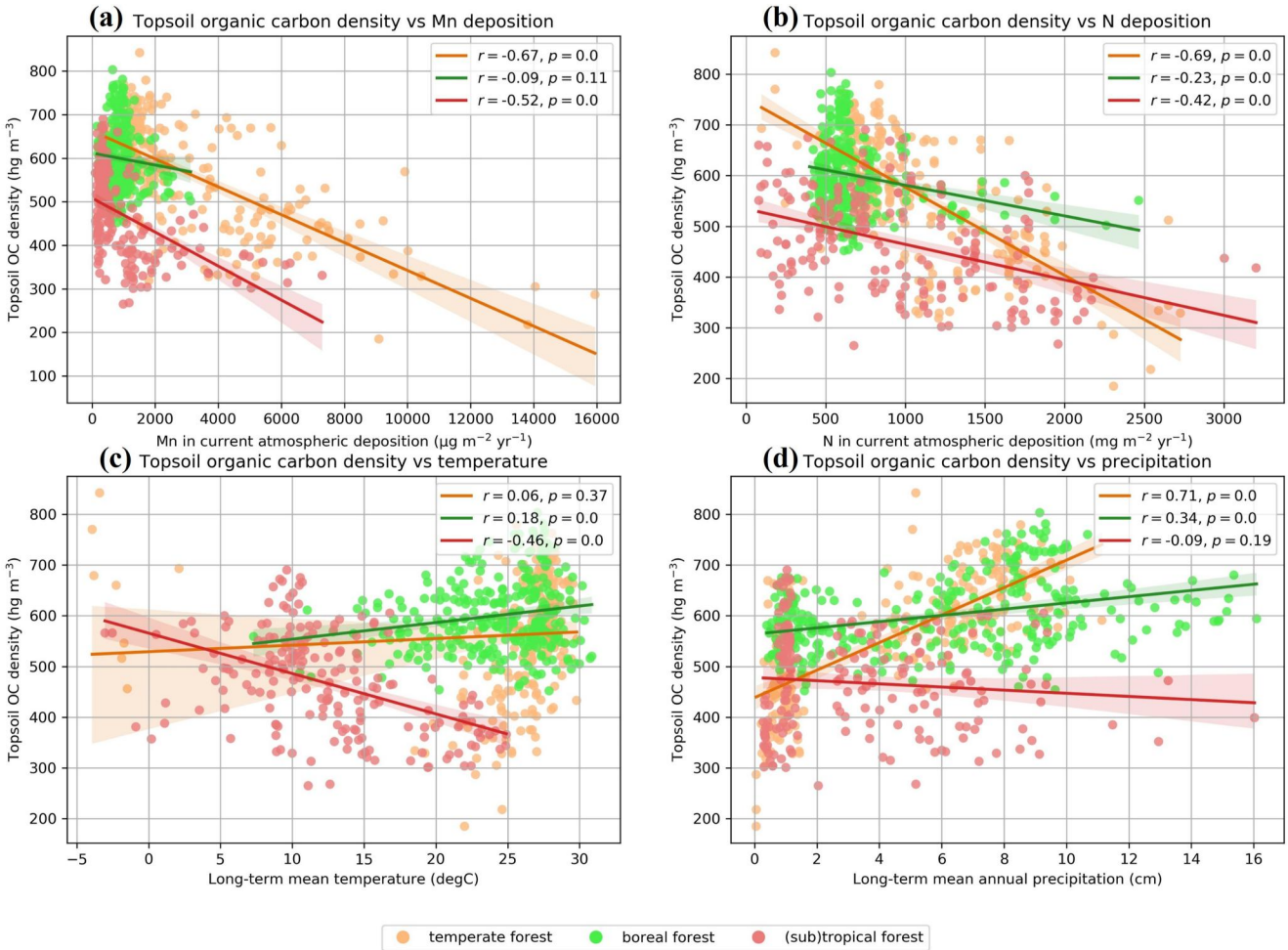

Figure 9. Scatter plots with simple linear regression lines between topsoil (0–5 cm) C density (hg m^{-3}) and (a) Mn in current atmospheric deposition (μg m^{-2} $year^{-1}$), (b) N in current atmospheric deposition (mg m^{-2} $year^{-1}$), (c) long-term mean temperature (°C), and (d) long-term mean annual precipitation (cm) in temperate, boreal, and tropical forests. "$p = 0.0$" legend suggests a p-value <0.0001.

Table 2
Result Statistics of Simple and Multilinear Regression Between Topsoil C Content and Mn Deposition, N Deposition, Temperature, and Precipitation

	Simple linear regression		Multilinear regression		
Variable name	r	p-value	coef	t	$P > \|t\|$
Intercept			500.2603	39.248	0.000
Mn deposition	−0.391	<0.0001	−0.0114	−4.738	0.000
N deposition	−0.493	<0.0001	−0.0661	−7.505	0.000
Temperature	0.270	<0.0001	4.1114	9.371	0.000
Precipitation	0.472	<0.0001	8.9193	10.031	0.000

4. Discussion

4.1. Model-Observation Discrepancy

Although our model simulation results had a moderately good representation of the atmospheric observations under the best estimate scenario, many stations were still under- or over-predicted (Figures 3 and 4). The discrepancy between the model and observations could arise from a variety of processes, with errors in the sources, deposition or transport pathways all contributing (Loosmore, 2003; Mahowald et al., 2011). For example, we were not able to include the emissions from direct volcanic eruptions due to the lack of data and thus constrained to apply non-eruptive degassing data only. Errors in estimates of dust deposition were thought to be of order of a factor of 10 (Mahowald et al., 2011). Because we derived Mn from industrial sources from a correlation with Fe (since these are the only spatially explicit mining emissions available: Rathod et al., 2020), emissions from nonferrous industries such as silico-manganese alloy, synthetic pyrolusite, and Mn chemical manufacturing plants were neglected (Parekh, 1990). Estimates of

fugitive emissions from mining were not available, and thus not included in this study.

Another limitation is that, except for desert and agricultural dust, we used a constant emission factor for each source because we did not have sufficient data to assess the spatial variability of the Mn emission factors from different sources such as PBP, sea sprays, and volcanoes, which could vary within the ranges given in Nriagu (1989). For example, trace element composition could vary in materials formed by biological production in different water masses (Kuss & Kremling, 1999). With the constant emission factor assumption, our model could over- or underestimate the observations, depending on the location of the site and its source apportionment.

While we found a negative correlation between topsoil C density and our simulated atmospheric Mn deposition in (sub)tropical and temperate forests, we did not find a relationship in boreal forests. These results are surprising given the observational findings from northern Swedish boreal forests, where Mn was found to act as a critical factor regulating C accumulation (Stendahl et al., 2017). This apparent discrepancy might be attributed to the limited number of soil observations within the boreal regime, introducing large uncertainty at the higher latitudes in our linear-interpolated soil map. With most soil observations located around the middle latitudes, it would not be surprising that we found stronger relationships than in the higher latitudes.

4.2. Limitations of the Observational Data

We collected atmospheric observations of Mn over six out of seven continents, but high spatial coverage was mostly restricted to industrialized countries. To improve our understanding of atmospheric contribution to the Mn cycle, more observations of the surface Mn concentration, especially in the coarse size fraction (as PM_{10} observations are much fewer than those of $PM_{2.5}$), in currently less-observed areas such as the higher latitudes are needed to further constrain the model. While the total concentration of PM is commonly monitored, it is the element-specific PM measurements that are more valuable to advancing our understanding of the trace-metal biogeochemical cycles.

Mn concentration in surface PM was chosen over direct Mn depositional observations for model calibration because of its higher data availability and timeliness. In addition, Mn deposition could be due to particles much larger than PM_{10} included here in the model. Herndon et al. (2011) made an effort to compile observations of Mn deposition, in which many of the reported values were collected in the past century, suitable for historical analysis and comparison but outdated for the tuning of a contemporary model, given that industrial emissions had decreased following environmental regulations in many countries. For example, our estimated Mn deposition was much smaller than the estimates given by Herndon et al. (2011) in the industrialized areas, while the natural components were more comparable. Another explanation for the difference is that direct depositional observations were usually close to the point emission source, whereas our model estimation was spatially averaged in each grid. As noted above, deposition data includes all size fractions, while here we consider only the size smaller than PM_{10}. Moreover, depositional observations are patchier and less systematically compiled; thus the number of them is insufficient for model tuning. However, direct depositional observations are important, and if having enough of them, atmospheric models like this could be tuned with depositional data as well. Therefore, there are still needs for more up-to-date field measurements of metal deposition by size fraction.

There are more locations with soil Mn measurements than atmospheric observations, but they are concentrated mostly in Europe and the U.S. Because of the uneven distribution of the soil observations and the limited number of them across many countries, we are not able to capture the variability of the soil Mn concentration at finer scales. For example, we did not include in our interpolation approach measurements of Mn concentration at metal-contaminated sites associated with mining or other industries (Lv et al., 2022), which could be patchy but important across industrialized regions (Herndon et al., 2011), having potential feedbacks on the reemission of the aerosols as dust. We suggest the value of more measurements on not only Mn, but also other trace elements in soils, especially in more developing countries, the higher latitudes, and the tropics. NCSS's soil characterization and USGS's geochemical and mineralogical survey of soils of the conterminous United States (D. B. Smith et al., 2013) can be proposed as model sampling campaigns which provide extensive and massive aerial coverage as well as highly compiled and sorted data sets.

Many studies (Baize, 2010; Okin et al., 2004; Wong et al., 2021) have suggested that soil orders, which are the highest level of taxonomic classification, are typically inadequate when dealing with trace element concentrations

in soils, because the intra-order variation is similar to the inter-order variation (Figure S8 in Supporting Information S1). Better estimation might be achieved with more refined classification at lower taxonomic levels such as suborders and great groups, or even quantitatively with particle size distribution. However, fewer sites specify the abovementioned information, and at such levels, the conversion between different classification systems is more complex.

4.3. Anthropogenic Perturbation and Implications for C Cycling

Our model and observations suggest that anthropogenic perturbations played an important role in global atmospheric Mn cycling, contributing about 31% of the total emissions. Anthropogenic sources were the dominant contributor of emissions in most industrialized regions, especially in the northern hemisphere (Figure 7) where they significantly accelerated Mn pseudo-turnover times in upper soils by enriching the atmospheric deposition in which the Mn-to-N ratio was boosted. Human activities, including industrialization and agricultural practices, likely alter Mn cycles by a factor of two or more in many associated areas (Figure 6), on the same order of magnitude as the perturbation to the cycling of other metals such as Mo, aluminum (Al), lead (Pb), mercury (Hg), and vanadium (V) (Rauch & Pacyna, 2009; Schlesinger et al., 2017; Selin, 2009; Sen & Peucker-Ehrenbrink, 2012; Wong et al., 2021).

The terrestrial ecological relevance of Mn deposition is how it modulates relationships between N deposition and soil C dynamics. Our results reinforce the negative correlation between Mn and topsoil C density in temperate forests globally (Kranabetter et al., 2021; Stendahl et al., 2017), suggesting Mn availability is likely a limiting factor in SOM decomposition. This implies that if atmospheric deposition is the major source of Mn in surficial soil layers, it has the potential to facilitate oxidative C decomposition by reducing Mn limitation, and in regions that are sensitive to anthropogenic activities, humans might indirectly alter the C cycle by releasing Mn-containing aerosols into the atmosphere through industrial and agricultural activities. While a significant proportion of global C is stored in the soils and vegetation of temperate forests (IPCC, 2000), increased C emissions from decomposition promoted by Mn addition could be important to global C dynamics and climate feedbacks, exacerbating the ongoing escalating C emissions subjected to wildfires (Phillips et al., 2022; B. Zhao et al., 2021). Furthermore, our correlation analysis indicates a negative Mn-C relationship in (sub)tropical forests in addition to temperate forests, where empirical relationships between Mn and soil C have been found. This calls for additional research into Mn deposition and its dynamics associated with soil C turnover in (sub)tropical forest ecosystems.

Most of the current studies of Mn-C dynamics measured total Mn concentration or extractable/available Mn from soils or litter layers, and very few considered the contribution of atmospheric deposition to surface soils. Direct field studies that correlate Mn deposition and C turnover would help determine the mechanisms behind the broad scale patterns predicted by our model. More field measurements and experimental studies are required to further quantify the influence of Mn deposition on C cycling. For example, our current understanding would be improved if SOM at different stages of decomposition could be distinguished. Berg et al. (2007) points out that Mn addition has a stronger effect on late-stage decomposition by enhancing lignin-degrading enzymes because microbes tend to decompose lignin after the more labile organic substrates (Berg, 2014; Berg & Matzner, 1997). In addition, we focused on modeling the total extractable and/or acid digested Mn in soils and atmospheric deposition and did not consider Mn bioavailability explicitly, which is crucial to the microorganisms that are responsible for decomposition and can be regulated by the cycling of Mn in different oxidation states (Keiluweit et al., 2015). Incorporation of mechanisms constraining the bioavailability, mobility, and reactivity of Mn (Keiluweit et al., 2015) in future model calibrations is essential for a more accurate interpretation. Finally, our estimated pseudo-turnover time and the Mn-to-N ratio could only partially represent the Mn status in soils because we did not include fluxes from other reservoirs in the Mn cycle. For instance, release of Mn(II) from clay mineral weathering and Mn(III, IV)-oxide reduction (Canfield et al., 2005) could increase the available Mn concentration in soils, creating the gap between the Mn-to-N ratio in deposition and in soils.

5. Conclusions

In this study, we present, for the first time, a spatially explicit estimation of global atmospheric Mn sources, distribution, and deposition using a combined model-observation approach. We estimate that anthropogenic sources (440 Gg Mn $year^{-1}$) represent approximately 31% of the total atmospheric Mn budget (1,400 Gg Mn

year^{-1}). Including this portion of Mn emissions in the model enhanced Mn deposition in many industrialized regions, which could accelerate soil Mn turnover as high as 100-fold and boost the Mn-to-N ratio in atmospheric deposition. Deposition of anthropogenic Mn from human activities has a high potential to facilitate SOM decomposition in temperate and (sub)tropical forest ecosystems, thus influencing C storage and the global C cycle. Given the scarcity of observations and limited understanding of atmospheric Mn sources, uncertainties are high in these estimations. Additional atmospheric and soil observations across different landscapes will help refine our model and the quantification of global biogeochemical cycles of trace metals like Mn.

Data Availability Statement

Observational synthesis available in the supplemental materials, while model results are available at the Zenodo: Lu & Mahowald. (2023). https://zenodo.org/records/10582252.

Acknowledgments
NMM and LL would like to acknowledge the support of DOE Grant: DE-SC0021302. SR acknowledges the support of Grants AEROEXTREME PID2021-125669NB-I00, AEROATLAN CGL 2015-66299-P & POLLINDUST CGL2011-26259 funded by ERDF and the Research State Agency of Spain.

References

Abanda, P. A., Compton, J. S., & Hannigan, R. E. (2011). Soil nutrient content, above-ground biomass and litter in a semi-arid shrubland, South Africa. *Geoderma*, *164*(3–4), 128–137. https://doi.org/10.1016/j.geoderma.2011.05.015

Adebiyi, A., Kok, J. F., Murray, B. J., Ryder, C. L., Stuut, J.-B. W., Kahn, R. A., et al. (2023). A review of coarse mineral dust in the Earth system. *Aeolian Research*, *60*, 100849. https://doi.org/10.1016/j.aeolia.2022.100849

Ahlgren, N. A., Nobel, A., Patton, A. P., Roache-Johnson, K., Jackson, L., Robinson, D., et al. (2014). The unique trace metal and mixed layer conditions of the Costa Rica upwelling dome support a distinct and dense community of Synechococcus. *Limnology and Oceanography*, *59*(6), 2166–2184. https://doi.org/10.4319/lo.2014.59.6.2166

Alastuey, A., Querol, X., Aas, W., Lucarelli, F., Pérez, N., Moreno, T., et al. (2016). Geochemistry of PM_{10} over Europe during the EMEP intensive measurement periods in summer 2012 and winter 2013. *Atmospheric Chemistry and Physics*, *16*(10), 6107–6129. https://doi.org/10.5194/acp-16-6107-2016

Albani, S., Mahowald, N. M., Perry, A. T., Scanza, R. A., Zender, C. S., Heavens, N. G., et al. (2014). Improved dust representation in the Community Atmosphere Model. *Journal of Advances in Modelling Earth Systems*, *6*(3), 541–570. https://doi.org/10.1002/2013MS000279

Alfaro, M. R., Montero, A., Ugarte, M. O., do Nascimento, C. W. A., de Aguiar Accioly, A. M., Biondi, C. M., & da Silva, Y. J. (2015). Background concentrations and reference values for heavy metals in soils of Cuba. *Environmental Monitoring and Assessment*, *187*(1), 4198. https://doi.org/10.1007/s10661-014-4198-3

Alongi, D. M., Wattayakorn, G., Boyle, S., Tirendi, F., Payn, C., & Dixon, P. (2004). Influence of roots and climate on mineral and trace element storage and flux in tropical mangrove soils. *Biogeochemistry*, *69*(1), 105–123. https://doi.org/10.1023/B:BIOG.0000031043.06245.af

Alves, C., Gonçalves, C., Fernandes, A. P., Tarelho, L., & Pio, C. (2011). Fireplace and woodstove fine particle emissions from combustion of western Mediterranean wood types. *Atmospheric Research*, *101*(3), 692–700. https://doi.org/10.1016/j.atmosres.2011.04.015

Andela, N., Morton, D. C., Giglio, L., Chen, Y., van der Werf, G. R., Kasibhatla, P. S., et al. (2017). A human-driven decline in global burned area. *Science*, *356*(6345), 1356–1362. https://doi.org/10.1126/science.aal4108

Andreae, T. W., Andreae, M. O., Ichoku, C., Maenhaut, W., Cafmeyer, J., Karnieli, A., & Orlovsky, L. (2002). Light scattering by dust and anthropogenic aerosol at a remote site in the Negev desert, Israel. *Journal of Geophysical Research*, *107*(D2), 4008. https://doi.org/10.1029/2001JD900252

Andruszczak, E. (1975). Zawartość makro- i mikroelementów w glebach i roślinności użytków rolnych Kotliny Kłodzkiej. *Roczniki Gleboznawcze*, *26*(3), 89–119.

Arditsoglou, A., Petaloti, C., Terzi, E., Sofoniou, M., & Samara, C. (2004). Size distribution of trace elements and polycyclic aromatic hydrocarbons in fly ashes generated in Greek lignite-fired power plants. *Science of the Total Environment*, *323*(1–3), 153–167. https://doi.org/10.1016/j.scitotenv.2003.10.013

Arimoto, R., Duce, R. A., Ray, B. J., & Tomza, U. (2003). Dry deposition of trace elements to the western North Atlantic. *Global Biogeochemical Cycles*, *17*(1), 1010. https://doi.org/10.1029/2001GB001406

Arimoto, R., Kim, Y. J., Kim, Y. P., Quinn, P. K., Bates, T. S., Anderson, T. L., et al. (2006). Characterization of Asian Dust during ACE-Asia. *Global and Planetary Change*, *52*(1–4), 23–56. https://doi.org/10.1016/j.gloplacha.2006.02.013

Artaxo, P., Martins, J. V., Yamasoe, M. A., Procopio, A. S., Pauliquevis, T. M., Andreae, M. O., et al. (2002). Physical and chemical properties of aerosols in the wet and dry seasons in Rondonia, Amazonia. *Journal of Geophysical Research*, *107*(D20), 8081. https://doi.org/10.1029/2001JD0000666

Asawalam, D. O., & Johnson, S. (2007). Physical and chemical characteristics of soils modified by earthworms and termites. *Communications in Soil Science and Plant Analysis*, *38*(3–4), 513–521. https://doi.org/10.1080/00103620601174569

Atanacio, A. J., & Cohen, D. D. (2020). The IAEA/RCA fine and coarse PMF receptor fingerprint database, Sydney, Australia: Australian Nuclear Science and Technology Organisation. Retrieved from http://www.ansto.gov.au/aspdatabases

Baize, D. (2010). *Concentrations of trace elements in soils: The three keys*. IUSS-International Union of Soil Sciences. Retrieved from https://www.researchgate.net/publication/275645543

Barraza, F., Lambert, F., Jorquera, H., Villalobos, A. M., & Gallardo, L. (2017). Temporal evolution of main ambient $PM_{2.5}$ sources in Santiago, Chile, from 1998 to 2012. *Atmospheric Chemistry and Physics*, *17*(16), 10093–10107. https://doi.org/10.5194/acp-17-10093-2017

Becquer, T., Quantin, C., & Boudot, J. P. (2010). Toxic levels of metals in Ferralsols under natural vegetation and crops in New Caledonia. *European Journal of Soil Science*, *61*(6), 994–1004. https://doi.org/10.1111/j.1365-2389.2010.01294.x

Berg, B. (2000). Litter decomposition and organic matter turnover in northern forest soils. *Forest Ecology and Management*, *133*(1–2), 13–22. https://doi.org/10.1016/S0378-1127(99)00294-7

Berg, B. (2014). Decomposition patterns for foliar litter – A theory for influencing factors. *Soil Biology and Biochemistry*, *78*, 222–232. https://doi.org/10.1016/j.soilbio.2014.08.005

Berg, B., Davey, M. P., de Marco, A., Emmett, B., Faituri, M., Hobbie, S. E., et al. (2010). Factors influencing limit values for pine needle litter decomposition: A synthesis for boreal and temperate pine forest systems. *Biogeochemistry*, *100*(1), 57–73. https://doi.org/10.1007/s10533-009-9404-y

Berg, B., & Matzner, E. (1997). Effect of N deposition on decomposition of plant litter and soil organic matter in forest systems. *Environmental Reviews*, *5*(1), 1–25. https://doi.org/10.1139/a96-017

Berg, B., Steffen, K. T., & McClaugherty, C. (2007). Litter decomposition rate is dependent on litter Mn concentrations. *Biogeochemistry*, *82*(1), 29–39. https://doi.org/10.1007/s10533-006-9050-6

Bergametti, G., Gomes, L., Doude-Gaussen, G., Rognon, P., & LeCoustumer, M. N. (1989). African dust observed over the Canary Islands: Source-regions identification and the transport pattern for some summer situations. *Journal of Geophysical Research*, *94*(D12), 14855–14864. https://doi.org/10.1029/jd094id12p14855

Beygi, M., & Jalali, M. (2018). Background levels of some trace elements in calcareous soils of the Hamedan Province, Iran. *Catena*, *162*, 303–316. https://doi.org/10.1016/j.catena.2017.11.001

Bibak, A., Moberg, J. P., & Borggaard, O. K. (1994). Content and distribution of cobalt, copper, manganese and molybdenum in Danish spodosols and ultisols. *Acta Agriculturae Scandinavica, Section B — Soil & Plant Science*, *44*(4), 208–213. https://doi.org/10.1080/09064719409410247

Block, C., & Dams, R. (1976). Study of fly ash emission during combustion of coal. *Environmental Science & Technology*, *10*(10), 1011–1017. https://doi.org/10.1021/es60121a013

Boente, C., Matanzas, N., García-González, N., Rodríguez-Valdés, E., & Gallego, J. R. (2017). Trace elements of concern affecting urban agriculture in industrialized areas: A multivariate approach. *Chemosphere*, *183*, 546–556. https://doi.org/10.1016/j.chemosphere.2017.05.129

Bond, T. C., Streets, D. G., Yarber, K. F., Nelson, S. M., Woo, J. H., & Klimont, Z. (2004). A technology-based global inventory of black and organic carbon emissions from combustion. *Journal of Geophysical Research*, *109*(D14), D14203. https://doi.org/10.1029/2003JD003697

Boucher, O., Randall, D., Artaxo, P., Bretherton, C., Feingold, G., Forster, P., et al. (2013). Clouds and aerosols. In T. F. Stocker, D. Qin, G.-K. Plattner, M. Tignor, S. K. Allen, J. Doschung, et al. (Eds.), *Climate change 2013: The physical science basis. Contribution of Working Group I to the fifth assessment report of the Intergovernmental Panel on Climate Change* (pp. 571–657). Cambridge University Press. https://doi.org/10.1017/CBO9781107415324.016

Bozlaker, A., Buzcu-Güven, B., Fraser, M., & Chellam, S. (2013). Insights into PM_{10} sources in Houston, Texas: Role of petroleum refineries in enriching lanthanoid metals during episodic emission events. *Atmospheric Environment*, *69*, 109–117. https://doi.org/10.1016/j.atmosenv.2012.11.068

Bozlaker, A., Prospero, J. M., Price, J., & Chellam, S. (2019). Identifying and quantifying the impacts of advected North African Dust on the concentration and composition of airborne fine particulate matter in Houston and Galveston, Texas. *Journal of Geophysical Research: Atmospheres*, *124*(22), 12282–12300. https://doi.org/10.1029/2019JD030792

Bradford, G. R., Chang, A. C., Page, A. L., Bakhtar, D., Frampton, J. A., & Wright, H. (1996). *Kearney foundation special report: Background concentrations of trace and major elements in California soils*. Kearney Foundation of Soil Science, Division of Agriculture and Natural Resources, University of California.

Brahney, J., Mahowald, N., Ward, D. S., Ballantyne, A. P., & Neff, J. C. (2015). Is atmospheric phosphorus pollution altering global alpine Lake stoichiometry? *Global Biogeochemical Cycles*, *29*(9), 1369–1383. https://doi.org/10.1002/2015GB005137

Brantley, S. L., & White, A. F. (2009). Approaches to modeling weathered regolith in thermodynamics and kinetics of water-rock interaction. In E. H. Oelkers & J. Schott (Eds.), *Reviews in mineralogy and geochemistry* (Vol. 70, pp. 435–484).

Browning, T. J., Achterberg, E. P., Engel, A., & Mawji, E. (2021). Manganese co-limitation of phytoplankton growth and major nutrient drawdown in the Southern Ocean. *Nature Communications*, *12*(1), 884. https://doi.org/10.1038/s41467-021-21122-6

Buccolieri, A., Buccolieri, G., Dell'Atti, A., Strisciullo, G., & Gagliano-Candela, R. (2010). Monitoring of total and bioavailable heavy metals concentration in agricultural soils. *Environmental Monitoring and Assessment*, *168*(1), 547–560. https://doi.org/10.1007/s10661-009-1133-0

Bullard, J., Baddock, M., McTainsh, G., & Leys, J. (2008). Sub-basin scale dust source geomorphology detected using MODIS. *Geophysical Research Letters*, *35*(15), L15404. https://doi.org/10.1029/2008GL033928

Burrows, S. M., Elbert, W., Lawrence, M. G., & Poschl, U. (2009). Bacteria in the global atmosphere--Part 1: Review and synthesis of literature for different ecosystems. *Atmospheric Chemistry and Physics*, *9*(23), 9263–9280. https://doi.org/10.5194/acp-9-9263-2009

Burt, R., Weber, T., Park, S., Yochum, S., & Ferguson, R. (2011). Trace element concentration and speciation in selected mining-contaminated soils and water in Willow Creek Floodplain, Colorado. *Applied and Environmental Soil Science*, *2011*, 237071. https://doi.org/10.1155/2011/237071

Cabrera, F., Clemente, L., Barrientos, E. D., Lopez, R., & Murillo, J. (1999). Heavy metal pollution of soils affected by the Guadiamar toxic flood. *Science of the Total Environment*, *242*(1–3), 117–129. https://doi.org/10.1016/S0048-9697(99)00379-4

Cancela, R. C., de Abreu, C. A., & Paz-Gonzalez, A. (2002). DTPA and Mehlich-3 micronutrient extractability in natural soils. *Communications in Soil Science and Plant Analysis*, *33*(15–18), 2879–2893. https://doi.org/10.1081/CSS-120014488

Canfield, D. E., Kristensen, E., & Thamdrup, B. (2005). The iron and manganese cycles. In *Advances in marine biology* (Vol. 48, pp. 269–312). Elsevier. https://doi.org/10.1016/S0065-2881(05)48008-6

Cassol, J. C., Pletsch, A. L., Costa Júnior, I. L., Bocardi, J., Alovisil, A. M. T., & Fronza, F. L. (2020). Natural contents of metals in soils from basaltic origins in western Parana, Brazil. *Revista Brasileira de Ciências Agrárias*, *15*(2), 1–7. https://doi.org/10.5039/agraria.v15i2a6992

Cavallari, J. M., Eisen, E. A., Fang, S. C., Schwartz, J., Hauser, R., Herrick, R. F., & Christiani, D. C. (2008). $PM_{2.5}$ metal exposures and nocturnal heart rate variability: A panel study of boilermaker construction workers. *Environmental Health: A Global Access Science Source*, *7*(1), 36. https://doi.org/10.1186/1476-069X-7-36

Chen, J. S., Wei, F. S., Zheng, C. J., Wu, Y. Y., & Adriano, D. C. (1991). Background concentrations of elements in soils of China. *Water, Air, & Soil Pollution*, *57*(8), 699–712. https://doi.org/10.1007/BF00282934

Chen, M., Ma, L. Q., & Harris, W. G. (1999). Baseline concentrations of 15 trace elements in Florida surface soils. *Journal of Environmental Quality*, *28*(4), 1173–1181. https://doi.org/10.2134/jeq1999.00472425002800040018x

Chen, M., Ma, L. Q., & Li, Y. C. (2000). Concentrations of P, K, Al, Fe, Mn, Cu, Zn, and As in marl soils from south Florida. *Annual Proceedings Soil and Crop Science Society of Florida*, *59*, 124–129.

Chen, Y., Street, J., & Paytan, A. (2006). Comparison between pure-water- and seawater-soluble nutrient concentrations of aerosols from the Gulf of Aqaba. *Marine Chemistry*, *101*(1–2), 141–152. https://doi.org/10.1016/j.marchem.2006.02.002

China, S., Veghte, D., Ahkami, A. H., Weis, J., Jansson, C., Guenther, A. B., et al. (2020). Microanalysis of primary biological particles from model grass over its life cycle. *ACS Earth and Space Chemistry*, *4*(10), 1895–1905. https://doi.org/10.1021/acsearthspacechem.0c00144

Chuang, P., Duvall, R., Shafer, M., & Schauer, J. (2005). The origin of water soluble particulate iron in the Asian atmospheric outflow. *Geophysical Research Letters*, *32*(7), L07813. https://doi.org/10.1029/2004GL021946

Cohen, D., Garton, D., Stelcer, E., Hawas, O., Wang, T., Pon, S., et al. (2004). Multielemental analysis and characterization of fine aerosols at several key ACE-Asia sites. *Journal of Geophysical Research*, *109*(D19), D19S12. https://doi.org/10.1029/2003JD003569

Computational and Information Systems Laboratory. (2019). *Cheyenne: HPE/SGI ICE XA System (NCAR Community Computing)*. National Center for Atmospheric Research. https://doi.org/10.5065/D6RX99HX

Córdoba, P., Ochoa-Gonzalez, R., Font, O., Izquierdo, M., Querol, X., Leiva, C., et al. (2012). Partitioning of trace inorganic elements in a coal-fired power plant equipped with a wet Flue Gas Desulphurisation system. *Fuel*, *92*(1), 145–157. https://doi.org/10.1016/j.fuel.2011.07.025

Dantu, S. (2010a). Factor analysis applied to a geochemical study of soils from parts of Medak and Sangareddy areas, Medak district, Andhra Pradesh, India. *Environmental Monitoring and Assessment*, *162*(1–4), 139–152. https://doi.org/10.1007/s10661-009-0782-3

Dantu, S. (2010b). Geochemical patterns in soils in and around Siddipet, Medak District, Andhra Pradesh, India. *Environmental Monitoring and Assessment*, *170*(1–4), 681–701. https://doi.org/10.1007/s10661-009-1267-0

Darwish, M. A. G., & Poellmann, H. (2015). Trace elements assessment in agricultural and desert soils of Aswan area, south Egypt: Geochemical characteristics and environmental impacts. *Journal of African Earth Sciences*, *112*(A), 358–373. https://doi.org/10.1016/j.jafrearsci.2015.06.018

da Silva, Y. J. A. B., do Nascimento, C. W. A., Cantalice, J. R. B., da Silva, Y. J. A. B., & Cruz, C. M. C. A. (2015). Watershed-scale assessment of background concentrations and guidance values for heavy metals in soils from a semiarid and coastal zone of Brazil. *Environmental Monitoring and Assessment*, *187*(9), 558. https://doi.org/10.1007/s10661-015-4782-1

da Silva Costa, R. D., Paula Neto, P., Costa Campos, M. C., do Nascimento, W. B., do Nascimento, C. W., Silva, L. S., & da Cunha, J. M. (2017). Natural contents of heavy metals in soils of the southern Amazonas state, Brazil. *Semina-Ciencias Agrarias*, *38*(6), 3499–3513. https://doi.org/10.5433/1679-0359.2017v38n6p3499

Davey, M. P., Berg, B., Emmett, B. A., & Rowland, P. (2007). Decomposition of oak leaf litter is related to initial litter Mn concentrations. *Canadian Journal of Botany*, *85*(1), 16–24. https://doi.org/10.1139/b06-150

Davies-Barnard, T., & Friedlingstein, P. (2020). The global distribution of biological nitrogen fixation in terrestrial natural ecosystems. *Global Biogeochemical Cycles*, *34*(3), e2019GB006387. https://doi.org/10.1029/2019GB006387

Davison, R. L., Natusch, D. F. S., Wallace, J. R., & Evans, C. A. (1974). Trace elements in fly ash. Dependence of concentration on particle size. *Environmental Science & Technology*, *8*(13), 1107–1113. https://doi.org/10.1021/es60098a003

Desboeufs, K. V., Sofikitis, A., Losno, R., Colin, J. L., & Ausset, P. (2005). Dissolution and solubility of trace metals from natural and anthropogenic aerosol particulate matter. *Chemosphere*, *58*(2), 195–203. https://doi.org/10.1016/j.chemosphere.2004.02.025

de Souza, C. A. C., Machado, A. T., Lima, L. R. P. D. A., & Cardoso, R. J. C. (2010). Stabilization of electric-arc furnace dust in concrete. *Materials Research*, *13*(4), 513–519. https://doi.org/10.1590/S1516-14392010000400014

de Souza, J. J., Pereira Abrahao, W. A., de Mello, J. W., da Silva, J., da Costa, L. M., & de Oliveira, T. S. (2015). Geochemistry and spatial variability of metal(loid) concentrations in soils of the state of Minas Gerais, Brazil. *Science of the Total Environment*, *505*, 338–349. https://doi.org/10.1016/j.scitotenv.2014.09.098

Després, V. R., Huffman, J. A., Burrows, S. M., Hoose, C., Safatov, A. S., Buryak, G., et al. (2012). Primary biological aerosol particles in the atmosphere: A review. *Tellus B: Chemical and Physical Meteorology*, *64*(1), 15598. https://doi.org/10.3402/tellusb.v64i0.15598

DFM & WSP. (2020). *Diagnóstico de Riesgo Ambiental, Región de Antofagasta, Componente A) Estudio de calidad de aire por la presencia de material particulado sedimentable en la ciudad de Antofagasta*. Ministry of Environment.

Dolan, R., Vanloon, J., Templeton, D., & Paudyn, A. (1990). Assessment of ICP-MS for routine multielement analysis of soil samples in environmental trace-element studies. *Fresenius Journal of Analytical Chemistry*, *336*(2), 99–105. https://doi.org/10.1007/BF00322545

do Nascimento, C. W., Lima, L. H. V., da Silva, F. L., Biondi, C. M., & Campos, M. C. C. (2018). Natural concentrations and reference values of heavy metals in sedimentary soils in the Brazilian Amazon. *Environmental Monitoring and Assessment*, *190*(10), 606. https://doi.org/10.1007/s10661-018-6989-4

Dongarrà, G., Manno, E., Varrica, D., & Vultaggio, M. (2007). Mass levels, crustal component and trace elements in PM_{10} in Palermo, Italy. *Atmospheric Environment*, *41*(36), 7977–7986. https://doi.org/10.1016/j.atmosenv.2007.09.015

Dongarrà, G., Manno, E., Varrica, D., & Vultaggio, M. (2010). Study on ambient concentrations of PM_{10}, $PM_{10\text{-}2.5}$, $PM_{2.5}$ and gaseous pollutants. Trace elements and chemical speciation of atmospheric particulates. *Atmospheric Environment*, *44*(39), 5244–5257. https://doi.org/10.1016/j.atmosenv.2010.08.041

Dreher, K. L., Jaskot, R. H., Lehmann, J. R., Richards, J. H., McGee, J. K., Ghio, A. J., & Costa, D. L. (1997). Soluble transition metals mediate residual oil fly ash induced acute lung injury. *Journal of Toxicology and Environmental Health*, *50*(3), 285–305. https://doi.org/10.1080/009841097160492

European Monitoring and Evaluation Programme. (2020). Retrieved from https://www.emep.int/

Expósito, A., Markiv, B., Ruiz-Azcona, L., Santibáñez, M., & Fernández-Olmo, I. (2021). Personal inhalation exposure to manganese and other trace metals in an environmentally exposed population: Bioaccessibility in size-segregated particulate matter samples. *Atmospheric Pollution Research*, *12*(8), 101123. https://doi.org/10.1016/j.apr.2021.101123

Fernandes, A. R., de Souza, E. S., de Souza Braz, A. M., Birani, S. M., & Alleoni, L. R. F. (2018). Quality reference values and background concentrations of potentially toxic elements in soils from the Eastern Amazon, Brazil. *Journal of Geochemical Exploration*, *190*, 453–463. https://doi.org/10.1016/j.gexplo.2018.04.012

Foulds, W. (1993). Nutrient concentrations of Foliage and soil in south-western Australia. *New Phytologist*, *125*(3), 529–546. https://doi.org/10.1111/j.1469-8137.1993.tb03901.x

Franklin, R. E., Duis, L., Smith, B. R., Brown, R., & Toler, J. E. (2003). Elemental concentrations in soils of South Carolina. *Soil Science*, *168*(4), 280–291. https://doi.org/10.1097/00010694-200304000-00005

Frey, S. D., Ollinger, S., Nadelhoffer, K., Bowden, R., Brzostek, E., Burton, A., et al. (2014). Chronic nitrogen additions suppress decomposition and sequester soil carbon in temperate forests. *Biogeochemistry*, *121*(2), 305–316. https://doi.org/10.1007/s10533-014-0004-0

Fuzzi, S., Decesari, S., Facchini, M. C., Cavalli, F., Emblico, L., Mircea, M., et al. (2007). Overview of the inorganic and organic composition of size-segregated aerosol in Rondônia, Brazil, from the biomass-burning period to the onset of the wet season. *Journal of Geophysical Research*, *112*(D1), D01201. https://doi.org/10.1029/2005JD006741

Gelaro, R., McCarty, W., Suárez, M. J., Todling, R., Molod, A., Takacs, L., et al. (2017). The modern-era retrospective analysis for research and applications, version 2 (MERRA-2). *Journal of Climate*, *30*(13), 5419–5454. https://doi.org/10.1175/JCLI-D-16-0758.1

Ghaemi, Z., Karbassi, A. R., Moattar, F., Hassani, A., & Khorasani, N. (2015). Evaluating soil metallic pollution and consequent human health hazards in the vicinity of an industrialized zone, case study of Mubarakeh steel complex, Iran. *Journal of Environmental Health Science and Engineering*, *13*(1), 75. https://doi.org/10.1186/s40201-015-0231-x

Gianini, M. F. D., Fischer, A., Gehrig, R., Ulrich, A., Wichser, A., Piot, C., et al. (2012). Comparative source apportionment of PM_{10} in Switzerland for 2008/2009 and 1998/1999 by positive matrix factorisation. *Atmospheric environment*, *54*, 149–158. https://doi.org/10.1016/j.atmosenv.2012.02.036

Gianini, M. F. D., Gehrig, R., Fischer, A., Ulrich, A., Wichser, A., & Hueglin, C. (2012). Chemical composition of PM_{10} in Switzerland: An analysis for 2008/2009 and changes since 1998/1999. *Atmospheric Environment*, *54*, 97–106. https://doi.org/10.1016/j.atmosenv.2012.02.037

Ginoux, P., Prospero, J., Gill, T. E., Hsu, N. C., & Zhao, M. (2012). Global scale attribution of anthropogenic and natural dust sources and their emission rates based on MODIS deep blue aerosol products. *Reviews of Geophysics*, *50*(3), RG3005. https://doi.org/10.1029/2012RG000388

Hamilton, D. S., Perron, M. M. G., Bond, T. C., Bowie, A. R., Buchholz, R. R., Guieu, C., et al. (2022). Earth, wind, fire, and pollution: Aerosol nutrient sources and impacts on ocean biogeochemistry. *Annual Review of Marine Science*, *14*(1), 303–330. https://doi.org/10.1146/annurev-marine-031921-013612

Hamilton, D. S., Scanza, R. A., Feng, Y., Guinness, J., Kok, J. F., Li, L., et al. (2019). Improved methodologies for Earth system modelling of atmospheric soluble iron and observation comparisons using the Mechanism of Intermediate complexity for Modelling Iron (MIMI v1.0). *Geoscientific Model Development*, *12*(9), 3835–3862. https://doi.org/10.5194/gmd-12-3835-201

Hand, J. L., Gill, T. E., & Schichtel, B. A. (2017). Spatial and seasonal variability in fine mineral dust and coarse aerosol mass at remote sites across the United States. *Journal of Geophysical Research: Atmospheres*, *122*(5), 3080–3097. https://doi.org/10.1002/2016JD026290

Hand, J. L., Gill, T. E., & Schichtel, B. A. (2019). Urban and rural coarse aerosol mass across the United States: Spatial and seasonal variability and long-term trends. *Atmospheric Environment*, *218*, 117025. https://doi.org/10.1016/j.atmosenv.2019.117025

Hansen, H. K., Pedersen, A. J., Ottosen, L. M., & Villumsen, A. (2001). Speciation and mobility of cadmium in straw and wood combustion fly ash. *Chemosphere*, *45*(1), 123–128. https://doi.org/10.1016/S0045-6535(01)00026-1

Hansen, M. C., Potapov, P. V., Moore, R., Hancher, M., Turubanova, S. A., Tyukavina, A., et al. (2013). High-resolution global maps of 21st-century forest cover change. *Science*, *342*(6160), 850–853. https://doi.org/10.1126/science.1244693

Hartley, I. P., Hill, T. C., Chadburn, S. E., & Hugelius, G. (2021). Temperature effects on carbon storage are controlled by soil stabilisation capacities. *Nature Communications*, *12*(1), 6713. https://doi.org/10.1038/s41467-021-27101-1

Haynes, R. J., & Swift, R. S. (1991). Concentrations of extractable Cu, Zn, Fe and Mn in a group of soils as influenced by air-drying and oven-drying and rewetting. *Geoderma*, *49*(3–4), 319–333. https://doi.org/10.1016/0016-7061(91)90083-6

He, Q., & Walling, D. E. (1997). The distribution of fallout ^{137}Cs and ^{210}Pb in undisturbed and cultivated soils. *Applied Radiation and Isotopes*, *48*(5), 677–690. https://doi.org/10.1016/S0969-8043(96)00302-8

Heald, C., & Spracklen, D. (2009). Atmospheric budget of primary biological aerosol particles from fungal sources. *Geophysical Research Letters*, *36*(9), L09806. https://doi.org/10.1029/2009GL037493

Herndon, E. M., Jin, L., & Brantley, S. (2011). Soils reveal widespread manganese enrichment from industrial inputs. *Environmental Science & Technology*, *45*(1), 241–247. https://doi.org/10.1021/es102001w

Hofrichter, M. (2002). Review: Lignin conversion by manganese peroxidase (MnP). *Enzyme and Microbial Technology*, *30*(4), 454–466. https://doi.org/10.1016/S0141-0229(01)00528-2

Hsu, C. Y., Chiang, H. C., Lin, S. L., Chen, M. J., Lin, T. Y., & Chen, Y. C. (2016). Elemental characterization and source apportionment of PM_{10} and $PM_{2.5}$ in the western coastal area of central Taiwan. *Science of the Total Environment*, *541*, 1139–1150. https://doi.org/10.1016/j.scitotenv.2015.09.122

Hua, Z., Chun-ming, J., Yong-gang, X., & Qiang, M. (2013). Analysis on concentration, distribution and budgets of Mn and Zn in soybean by using ICP-AES. *Spectroscopy and Spectral Analysis*, *33*(4), 1112–1115. https://doi.org/10.3964/j.issn.1000-0593(2013)04-1112-04

Hueglin, C., Gehrig, R., Baltensperger, U., Gysel, M., Monn, C., & Vonmont, H. (2005). Chemical characterisation of $PM_{2.5}$, PM_{10} and coarse particles at urban, near-city and rural sites in Switzerland. *Atmospheric Environment*, *39*(4), 637–651. https://doi.org/10.1016/j.atmosenv.2004.10.027

Huffman, G. P., Huggins, F. E., Shah, N., Huggins, R., Linak, W. P., Miller, C. A., et al. (2000). Characterization of fine particulate matter produced by combustion of residual fuel oil. *Journal of the Air & Waste Management Association*, *50*(7), 1106–1114. https://doi.org/10.1080/10473289.2000.10464157

Hurrell, J. W., Holland, M. M., Gent, P. R., Chan, S., Kay, J. E., Kushner, P. J., et al. (2013). The Community Earth System Model: A framework for collaborative research. *Bulletin of the American Meteorological Society*, *94*(9), 1339–1360. https://doi.org/10.1175/BAMS-D-12-00121.1

Hurtt, G. C., Chini, L. P., Frolking, S., Betts, R. A., Feddema, J., Fischer, G., et al. (2011). Harmonization of land-use scenarios for the period 1500-2100: 600 years of global gridded annual land-use transitions, wood harvest, and resulting secondary lands. *Climatic Change*, *109*(1–2), 117–161. https://doi.org/10.1007/s10584-011-0153-2

Ikem, A., Campbell, M., Nyirakabibi, I., & Garth, J. (2008). Baseline concentrations of trace elements in residential soils from Southeastern Missouri. *Environmental Monitoring and Assessment*, *140*(1), 69–81. https://doi.org/10.1007/s10661-007-9848-2

Imran, M., Khan, A.-H., Aziz-ul-Hassan, Kanwal, F., Mitu, L., Amir, M., & Iqbal, M. A. (2010). Evaluation of physico-chemical characteristics of soil samples collected from Harrapa-Sahiwal (Pakistan). *Asian Journal of Chemistry*, *22*(6), 4823–4830.

Iñigo, V., Andrades, M., Alonso-Martirena, J. I., Marín, A., & Jiménez-Ballesta, R. (2011). Multivariate statistical and GIS-based approach for the identification of Mn and Ni concentrations and spatial variability in soils of a humid Mediterranean environment: La Rioja, Spain. *Water, Air, & Soil Pollution*, *222*(1), 271–284. https://doi.org/10.1007/s11270-011-0822-9

IPCC. (2000). *Special report on land use, land-use change, and forestry*. Cambridge University Press. Retrieved from https://www.ipcc.ch/report/land-use-land-use-change-and-forestry

Ivezic, V., Singh, B. R., Almas, A. R., & Loncaric, Z. (2011). Water extractable concentrations of Fe, Mn, Ni, Co, Mo, Pb and Cd under different land uses of Danube basin in Croatia. *Acta Agriculturae Scandinavica, Section B — Soil & Plant Science*, *61*(8), 747–759. https://doi.org/10.1080/09064710.2011.557392

Jahiruddin, M., Harada, H., Hatanaka, T., & Islam, M. R. (2000). Status of trace elements in agricultural soils of Bangladesh and relationship with soil properties. *Soil Science and Plant Nutrition*, *46*(4), 963–968. https://doi.org/10.1080/00380768.2000.10409161

Jang, H. N., Seo, Y. C., Lee, J. H., Hwang, K. W., Yoo, J. I., Sok, C. H., & Kim, S. H. (2007). Formation of fine particles enriched by V and Ni from heavy oil combustion: Anthropogenic sources and drop-tube furnace experiments. *Atmospheric Environment*, *41*(5), 1053–1063. https://doi.org/10.1016/j.atmosenv.2006.09.011

Jones, M. E., LaCroix, R. E., Zeigler, J., Ying, S. C., Nico, P. S., & Keiluweit, M. (2020). Enzymes, manganese, or iron? Drivers of oxidative organic matter decomposition in soils. *Environmental Science and Technology*, *54*(21), 14114–14123. https://doi.org/10.1021/acs.est.0c04212

Joshi, D., Srivastava, P. C., Dwivedi, R., Pachauri, S. P., & Shukla, A. K. (2017). Chemical fractions of Mn in acidic soils and selection of suitable soil extractants for assessing Mn availability to Maize (*Zea Mays* L.). *Communications in Soil Science and Plant Analysis*, *48*(8), 886–897. https://doi.org/10.1080/00103624.2017.1322601

Kanakidou, M., Myriokefalitakis, S., Daskalakis, N., Fanourgakis, G., Nenes, A., Baker, A. R., et al. (2016). Past, present, and future atmospheric nitrogen deposition. *Journal of the Atmospheric Sciences*, *73*(5), 2039–2047. https://doi.org/10.1175/JAS-D-15-0278.1

Kassaye, Y. A., Skipperud, L., Meland, S., Dadebo, E., Einset, J., & Salbu, B. (2012). Trace element mobility and transfer to vegetation within the Ethiopian Rift Valley lake areas. *Journal of Environmental Monitoring*, *14*(10), 2698–2709. https://doi.org/10.1039/c2em30271c

Kaste, J. M., Friedland, A. J., & Stürup, S. (2003). Using stable and radioactive isotopes to trace atmospherically deposited Pb in Montane forest soils. *Environmental Science & Technology*, *37*(16), 3560–3567. https://doi.org/10.1021/es026372k

Kauffman, J., Cummings, D. L., Ward, D. E., & Babbitt, R. (1995). Fire in the Brazilian Amazon: 1. Biomass, nutrient pools, and losses in slashed primary forests. *Oecologia*, *104*(4), 397–408. https://doi.org/10.1007/BF00341336

Keiluweit, M., Nico, P., Harmon, M. E., Mao, J., Pett-Ridge, J., & Kleber, M. (2015). Long-term litter decomposition controlled by manganese redox cycling. *Proceedings of the National Academy of Sciences of the United States of America*, *112*(38), E5253–E5260. https://doi.org/10.1073/pnas.1508945112

Kellogg, C. A., & Griffin, D. W. (2006). Aerobiology and the global transport of desert dust. *Trends in Ecology and Evolution*, *21*(11), 638–644. https://doi.org/10.1016/j.tree.2006.07.004

Kloss, S., Zehetner, F., Oburger, E., Jannis, B., Kitzler, B., Wenzel, W. W., et al. (2014). Trace element concentrations in leachates and mustard plant tissue (*Sinapis alba* L.) after biochar application to temperate soils. *Science of the Total Environment*, *481*, 498–508. https://doi.org/10.1016/j.scitotenv.2014.02.093

Kok, J. F., Albani, S., Mahowald, N. M., & Ward, D. S. (2014). An improved dust emission model – Part 2: Evaluation in the Community Earth System Model, with implications for the use of dust source functions. *Atmospheric Chemistry and Physics*, *14*(23), 13043–13061. https://doi.org/10.5194/acp-14-13043-2014

Kok, J. F., Mahowald, N. M., Fratini, G., Gillies, J. A., Ishizuka, M., Leys, J. F., et al. (2014). An improved dust emission model – Part 1: Model description and comparison against measurements. *Atmospheric Chemistry and Physics*, *14*(23), 13023–13041. https://doi.org/10.5194/acp14-13023-2014

Koukouzas, N., Hämäläinen, J., Papanikolaou, D., Tourunen, A., & Jäntti, T. (2007). Mineralogical and elemental composition of fly ash from pilot scale fluidised bed combustion of lignite, bituminous coal, wood chips and their blends. *Fuel*, *86*(14), 2186–2193. https://doi.org/10.1016/j.fuel.2007.03.036

Kranabetter, J. M., Philpott, T. J., & Dunn, D. E. (2021). Manganese limitations and the enhanced soil carbon sequestration of temperate rainforests. *Biogeochemistry*, *156*(2), 195–209. https://doi.org/10.1007/s10533-021-00840-5

Krawchuk, M. A., Moritz, M. A., Parisien, M. A., Van Dorn, J., & Hayhoe, K. (2009). Global pyrogeography: The current and future distribution of wildfire. *PLoS One*, *4*(4), e5102. https://doi.org/10.1371/journal.pone.0005102

Kuss, J., & Kremling, K. (1999). Spatial variability of particle associated trace elements in near-surface waters of the North Atlantic (30°N/60°W to 60°N/2°W), derived by large volume sampling. *Marine Chemistry*, *68*(1–2), 71–86. https://doi.org/10.1016/S0304-4203(99)00066-3

Kyllönen, K., Vestenius, M., Anttila, P., Makkonen, U., Aurela, M., Wängberg, I., et al. (2020). Trends and source apportionment of atmospheric heavy metals at a subarctic site during 1996-2018. *Atmospheric Environment*, *236*, 117644. https://doi.org/10.1016/j.atmosenv.2020.117644

Laing, J. R., Hopke, P. K., Hopke, E. F., Husain, L., Dutkiewicz, V. A., Paatero, J., & Viisanen, Y. (2014a). Long-term particle measurements in Finnish Arctic: Part I-Chemical composition and trace metal solubility. *Atmospheric Environment*, *88*, 275–284. https://doi.org/10.1016/j.atmosenv.2014.03.002

Laing, J. R., Hopke, P. K., Hopke, E. F., Husain, L., Dutkiewicz, V. A., Paatero, J., & Viisanen, Y. (2014b). Long-term particle measurements in Finnish Arctic: Part II-Trend analysis and source location identification. *Atmospheric Environment*, *88*, 285–296. https://doi.org/10.1016/j.atmosenv.2014.01.015

Lavado, R. S., & Porcelli, C. A. (2000). Contents and main fractions of trace elements in Typic Argiudolls of the Argentinean Pampas. *Chemical Speciation and Bioavailability*, *12*(2), 67–70. https://doi.org/10.3184/095422900782775553

Lawrence, D. M., Fisher, R. A., Koven, C. D., Oleson, K. W., Swenson, S. C., Bonan, G., et al. (2019). The Community Land Model Version 5: Description of new features, benchmarking, and impact of forcing uncertainty. *Journal of Advances in Modeling Earth Systems*, *11*(12), 4245–4287. https://doi.org/10.1029/2018MS001583

Li, L., Mahowald, N., Miller, R. L., Perez Garcia-Pando, C., Klose, M., Hamilton, D. S., et al. (2021). Quantifying the range of the dust direct radiative effect due to source mineralogy uncertainty. *Atmospheric Chemistry and Physics Discussions*, *21*(5), 3973–4005. https://doi.org/10.5194/acp-2020-547

Li, L., Mahowald, N. M., Kok, J. F., Liu, X., Wu, M., Leung, D. M., et al. (2022). Importance of different parameterization changes for the updated dust cycle modeling in the Community Atmosphere Model (version 6.1). *Geoscientific Model Development*, *15*(22), 8181–8219. https://doi.org/10.5194/gmd-15-8181-2022

Linak, W. P., Miller, C. A., & Wendt, J. O. L. (2000a). Fine particle emissions from residual fuel oil combustion: Characterization and mechanisms of formation. *Proceedings of the Combustion Institute*, *28*(2), 2651–2658. https://doi.org/10.1016/S0082-0784(00)80684-0

Linak, W. P., Miller, C. A., & Wendt, J. O. L. (2000b). Comparison of particle size distributions and elemental partitioning from the combustion of pulverized coal and residual fuel oil. *Journal of the Air & Waste Management Association*, *50*(8), 1532–1544. https://doi.org/10.1080/10473289.2000.10464171

Lindell, L., Astrom, M., & Oberg, T. (2010). Land-use versus natural controls on soil fertility in the Subandean Amazon, Peru. *Science of the Total Environment*, *408*(4), 965–975. https://doi.org/10.1016/j.scitotenv.2009.10.039

Liu, X., Easter, R. C., Ghan, S. J., Zaveri, R., Rasch, P., Shi, X., et al. (2011). Toward a minimal representation of aerosol direct and indirect effects: Model description and evaluation. *Geoscientific Model Development Discussions*, *4*(4), 3485–3598. https://doi.org/10.5194/gmdd-4-3485-2011

Liu, X., Ma, P. L., Wang, H., Tilmes, S., Singh, B., Easter, R. C., et al. (2016). Description and evaluation of a new four-mode version of the Modal Aerosol Module (MAM4) within version 5.3 of the Community Atmosphere Model. *Geoscientific Model Development*, *9*(2), 505–522. https://doi.org/10.5194/gmd-9-505-2016

Loosmore, G. A. (2003). Evaluation and development of models for resuspension of aerosols at short times after deposition. *Atmospheric Environment*, *37*(5), 639–647. https://doi.org/10.1016/S1352-2310(02)00902-0

Lu, L., & Mahowald, N. (2023). Model outputs for characterizing the atmospheric Mn cycle and its impact on terrestrial biogeochemistry [Dataset]. *Zenodo*. https://doi.org/10.5281/zenodo.10582252

Lv, Y., Kabanda, G., Chen, Y., Wu, C., & Li, W. (2022). Spatial distribution and ecological risk assessment of heavy metals in manganese (Mn) contaminated site. *Frontiers in Environmental Science*, *10*, 942544. https://doi.org/10.3389/fenvs.2022.942544

Ma, L. Q., Tan, F., & Harris, W. G. (1997). Concentrations and distributions of eleven metals in Florida soils. *Journal of Environmental Quality*, *26*(3), 769–775. https://doi.org/10.2134/jeq1997.00472425002600030025x

Machado, J., Brehm, F., Moraes, C., Santos, C., Vilela, A., & Cunha, J. (2006). Chemical, physical, structural and morphological characterization of the electric arc furnace dust. *Journal of Hazardous Materials*, *136*(3), 953–960. https://doi.org/10.1016/j.jhazmat.2006.01.044

Mackey, K. R. M., Hunter, D., Fischer, E. V., Jiang, Y., Allen, B., Chen, Y., et al. (2013). Aerosol-nutrient-induced picoplankton growth in Lake Tahoe. *Journal of Geophysical Research: Biogeosciences*, *118*(3), 1054–1067. https://doi.org/10.1002/jgrg.20084

Maenhaut, W., & Cafmeyer, J. (1998). Long-term atmospheric aerosol study at urban and rural sites in Belgium using multi-elemental analysis by particle-induced x-ray emission spectrometry and short-irradiation instrumental neutron activation analysis. *X-Ray Spectrometry*, *27*(4), 236–246. https://doi.org/10.1002/(SICI)1097-4539(199807/08)27:4<236::AID-XRS292>3.0.CO;2-F

Maenhaut, W., Cafmeyer, J., Ptasinski, J., Andreae, M. O., Andreae, T. W., Elbert, W., et al. (1997). Chemical composition and light scattering of the atmospheric aerosol at a remote site in the Negev desert, Israel. *Journal of Aerosol Science*, *28*(Suppl. 1), S73–S74. https://doi.org/10.1016/S0021-8502(97)85037-9

Maenhaut, W., De Ridder, D. J., Fernández-Jiménez, M. T., Hooper, M. A., Hooper, B., & Nurhayati, M. (2002). Long-term observations of regional aerosol composition at two sites in Indonesia. *Nuclear Instruments and Methods in Physics Research Section B: Beam Interactions With Materials and Atoms*, *189*(1–4), 259–265. https://doi.org/10.1016/S0168-583X(01)01054-0

Maenhaut, W., Fernández-Jiménez, M.-T., & Artaxo, P. (1999). Long-term study of atmospheric aerosols in Cuiabá, Brazil: Multielemental composition, sources and source apportionment. *Journal of Aerosol Science*, *30*(0021–8502), S259–S260. https://doi.org/10.1016/s0021-8502(99)80141-4

Maenhaut, W., Fernández-Jiménez, M.-T., Rajta, I., & Artaxo, P. (2002). Two-year study of atmospheric aerosols in Alta Floresta, Brazil: Multielemental composition and source apportionment. *Nuclear Instruments and Methods in Physics Research*, *B189*(1–4), 243–248. https://doi.org/10.1016/S0168-583X(01)01050-3

Maenhaut, W., Fernández-Jiménez, M.-T., Rajta, I., Dubtsov I, S., Meixner, F. X., Andreae, M. O., et al. (2000). Long-term aerosol composition measurements and source apportionment at Rukomechi, Zimbabwe. *Journal of Aerosol Science*, *31*(Suppl. 1), S228–S229. https://doi.org/10.1016/S0021-8502(00)90237-4

Maenhaut, W., Fernández-Jiménez, M. T., Vanderzalm, J. L., Hooper, B., Hooper, M. A., & Tapper, N. J. (2000). Aerosol composition at Jabiru, Australia, and impact of biomass burning. *Journal of Aerosol Science*, *31*(Suppl. 1), S745–S746. https://doi.org/10.1016/S0021-8502(00)90755-9

Maenhaut, W., Francois, F., Cafmeyer, J., Gilot, C., & Hanssen, J. (1997). Long-term aerosol study in southern Norway, and the relationship of aerosol components to source regions. In P. Borrell, P. Borrell, K. Kelly, T. Cvitas, & W. Seiler (Eds.), *Transport and transformation of pollutants in the troposphere: Proceedings of EUROTRAC symposium '96, vol. 1: Clouds, aerosols, modelling and photo-oxidants* (pp. 277–280). Computational Mechanics.

Maenhaut, W., Koppen, G., & Artaxo, P. (1996). Long-term atmospheric aerosol study in Cuiabá, Brazil: Multielemental composition, sources, and impact of biomass burning. *Biomass Burning and Global Change*, *2*, 637–652.

Maenhaut, W., Nava, S., Lucarelli, F., Wang, W., Chi, X., & Kulmala, M. (2011). Chemical composition, impact from biomass burning, and mass closure for $PM_{2.5}$ and PM_{10} aerosols at Hyytiälä, Finland, in summer 2007. *X-Ray Spectrometry*, *40*(3), 168–171. https://doi.org/10.1002/xrs.1302

Maenhaut, W., Raes, N., Chi, X., Cafmeyer, J., & Wang, W. (2008). Chemical composition and mass closure for $PM_{2.5}$ and PM_{10} aerosols at K-puszta, Hungary, in summer 2006. *X-Ray Spectrometry*, *37*(2), 193–197. https://doi.org/10.1002/xrs.1062

Maenhaut, W., Raes, N., Chi, X., Cafmeyer, J., Wang, W., & Salma, I. (2005). Chemical composition and mass closure for fine and coarse aerosols at a kerbside in Budapest, Hungary, in spring 2002. *X-Ray Spectrometry*, *34*(4), 290–296. https://doi.org/10.1002/xrs.820

Maenhaut, W., Salma, I., Cafmeyer, J., Annegarn, H. J., & Andreae, M. O. (1996). Regional atmospheric aerosol composition and sources in the eastern Transvaal, South Africa, and impact of biomass burning. *Journal of Geophysical Research*, *101*(D19), 23631–23650. https://doi.org/10.1029/95JD02930

Maenhaut, W., Salomonovic, R., Cafmeyer, J., Ichoku, C., Karnieli, A., & Andreae, M. O. (1996). Anthropogenic and natural radiatively active aerosol types at Sede Boker, Israel. *Journal of Aerosol Science*, *27*(Suppl. 1), S47–S48. https://doi.org/10.1016/0021-8502(96)00096-1

Mahowald, N. M., Albani, S., Kok, J. F., Engelstaeder, S., Scanza, R., Ward, D. S., & Flanner, M. G. (2014). The size distribution of desert dust aerosols and its impact on the Earth system. *Aeolian Research*, *15*, 53–71. https://doi.org/10.1016/j.aeolia.2013.09.002

Mahowald, N. M., Artaxo, P., Baker, A. R., Jickells, T. D., Okin, G. S., Randerson, J. T., & Townsend, A. R. (2005). Impacts of biomass burning emissions and land use change on Amazonian atmospheric phosphorus cycling and deposition. *Global Biogeochemical Cycles*, *19*(4), GB4030. https://doi.org/10.1029/2005GB002541

Mahowald, N. M., Engelstaedter, S., Luo, C., Sealy, A., Artaxo, P., Benitez-Nelson, C., et al. (2009). Atmospheric iron deposition: Global distribution, variability, and human perturbations. *Annual Review of Marine Science*, *1*, 245–278. https://doi.org/10.1146/annurev.marine.010908.163727

Mahowald, N. M., Hamilton, D. S., Mackey, K. R. M., Moore, J. K., Baker, A. R., Scanza, R. A., & Zhang, Y. (2018). Aerosol trace metal leaching and impacts on marine microorganisms. *Nature Communications*, *9*(1), 2614. https://doi.org/10.1038/s41467-018-04970-7

Mahowald, N. M., Ward, D. S., Kloster, S., Flanner, M. G., Heald, C. L., Heavens, N. G., et al. (2011). Aerosol impacts on climate and biogeochemistry. *Annual Review of Environment and Resources*, *36*(1), 45–74. https://doi.org/10.1146/annurev-environ-042009-094507

Malm, W., Pitchford, M., McDade, C., & Ashbaugh, L. (2007). Coarse particle speciation at selected locations in the rural continental United States. *Atmospheric Environment*, *41*(10), 2225–2239. https://doi.org/10.1016/j.atmosenv.2006.10.077

Mamane, Y., Miller, J. L., & Dzubay, T. G. (1986). Characterization of individual fly ash particles emitted from coal- and oil-fired power plants. *Atmospheric Environment (1967)*, *20*(11), 2125–2135. https://doi.org/10.1016/0004-6981(86)90306-9

Martinez-Tarazona, M., Palacios, J. M., Martinez-Alonso, A., & Tascon, J. (1990). The characterization of organomineral components of low-rank coals. *Fuel Processing Technology*, *25*(1), 81–87. https://doi.org/10.1016/0378-3820(90)90097-C

Mashi, S. A., Yaro, S. A., & Haiba, A. S. (2004). Cu, Mn, Fe, and Zn levels in soils of Shika area, Nigeria. *Biomedical and Environmental Sciences*, *17*(4), 426–431.

McKenzie, R. M. (1957). The distribution of trace elements in some South Australian red-brown earths. *Australian Journal of Agricultural Research*, *8*(3), 246–252. https://doi.org/10.1071/AR9570246

McNeill, J., Snider, G., Weagle, C. L., Walsh, B., Bissonnette, P., Stone, E., et al. (2020). Large global variations in measured airborne metal concentrations driven by anthropogenic sources. *Scientific Reports*, *10*(1), 21817. https://doi.org/10.1038/s41598-020-78789-y

Meij, R. (1994). Trace element behavior in coal-fired power plants. *Fuel Processing Technology*, *39*(1–3), 199–217. https://doi.org/10.1016/0378-3820(94)90180-5

Michopoulos, P., Economou, A., & Nikolis, N. (2004). Soil extractable manganese and uptake in a natural fir stand grown on calcareous soils. *Communications in Soil Science and Plant Analysis*, *35*(1–2), 233–241. https://doi.org/10.1081/CSS-120027646

Michopoulos, P., Farmaki, E., & Thomaidis, N. (2017). Foliar status and factors affecting foliar and soil chemistry in a natural aleppo pine forest. *Journal of Plant Nutrition*, *40*(10), 1443–1452. https://doi.org/10.1080/01904167.2016.1269341

Mikkonen, H. G., Clarke, B. O., Dasika, R., Wallis, C. J., & Reichman, S. M. (2017). Assessment of ambient background concentrations of elements in soil using combined survey and open-source data. *Science of the Total Environment*, *580*, 1410–1420. https://doi.org/10.1016/j.scitotenv.2016.12.106

Miko, S., Durn, G., Adamcova, R., Covic, M., Dubikova, M., Skalsky, R., et al. (2003). Heavy metal distribution in karst soils from Croatia and Slovakia. *Environmental Geology*, *45*(2), 262–272. https://doi.org/10.1007/s00254-003-0878-y

Mkoma, S. L. (2008). Physico-chemical characterisation of atmospheric aerosols in Tanzania, with emphasis on the carbonaceous aerosol components and on chemical mass closure. (Ph.D. Thesis) (p. 162). Ghent University. ISBN: 978-90-5989-230-9.

Mkoma, S. L., Maenhaut, W., Chi, X., Wang, W., & Raes, N. (2009a). Characterisation of PM_{10} atmospheric aerosols for the wet season 2005 at two sites in East Africa. *Atmospheric Environment*, *43*(3), 631–639. https://doi.org/10.1016/j.atmosenv.2008.10.008

Mkoma, S. L., Maenhaut, W., Chi, X., Wang, W., & Raes, N. (2009b). Chemical composition and mass closure for PM_{10} aerosols during the 2005 dry season at a rural site in Morogoro, Tanzania. *X-Ray Spectrometry*, *38*(4), 293–300. https://doi.org/10.1002/xrs.1179

Moore, J. A. M., Anthony, M. A., Pec, G. J., Trocha, L. K., Trzebny, A., Geyer, K. M., et al. (2021). Fungal community structure and function shifts with atmospheric nitrogen deposition. *Global Change Biology*, *27*(7), 1349–1364. https://doi.org/10.1111/gcb.15444

Moore, O. W., Curti, L., Woulds, C., Bradley, J. A., Babakhani, P., Mills, B. J. W., et al. (2023). Long-term organic carbon preservation enhanced by iron and manganese. *Nature*, *621*(7978), 312–317. https://doi.org/10.1038/s41586-023-06325-9

Morales Del Mastro, A., Londonio, A., Jimenez Rebagliati, R., Pereyra, M., Dawidowski, L., Gomez, D., & Smichowski, P. (2015). Plasma-based techniques applied to the determination of 17 elements in partitioned top soils. *Microchemical Journal*, *123*, 224–229. https://doi.org/10.1016/j.microc.2015.07.002

Morera-Gómez, Y., Elustondo, D., Lasheras, E., Alonso-Hernández, C. M., & Santamaría, J. M. (2018). Chemical characterization of PM_{10} samples collected simultaneously at a rural and an urban site in the Caribbean coast: Local and long-range source apportionment. *Atmospheric Environment*, *192*, 182–192. https://doi.org/10.1016/j.atmosenv.2018.08.058

Nalovic, L., & Pinta, M. (1969). Recherches sur les éléments traces dans les sols tropicaux: Étude de quelques sols de Madagascar. *Geoderma*, *3*(2), 117–132. https://doi.org/10.1016/0016-7061(69)90008-1

Nanzyo, M., Yamasaki, S.-I., & Honna, T. (2002). Changes in content of trace and ultratrace elements with an increase in noncrystalline materials in volcanic ash soils of Japan. *Clay Science*, *12*(1), 25–32. https://doi.org/10.11362/jcssjclayscience1960.12.25

Natali, S. M., Sañudo-wilhelmy, S. A., & Lerdau, M. T. (2009). Plant and soil mediation of elevated CO_2 impacts on trace metals. *Ecosystems*, *12*(5), 715–727. https://doi.org/10.1007/s10021-009-9251-7

Navas, A., & Lindhorfer, H. (2005). Chemical partitioning of Fe, Mn, Zn and Cr in mountain soils of the Iberian and Pyrenean ranges (NE Spain). *Soil and Sediment Contamination: An International Journal*, *14*(3), 249–259. https://doi.org/10.1080/15320380590928311

Nguyen, B. T., Do, T. K., van Tran, T., Dang, M. K., Dell, C. J., Luu, P. V., & Vo, Q. T. K. (2018). High soil Mn and Al, as well as low leaf P concentration, may explain for low natural rubber productivity on a tropical acid soil in Vietnam. *Journal of Plant Nutrition*, *41*(7), 903–914. https://doi.org/10.1080/01904167.2018.1431674

Njofang, C., Matschullat, J., Amougou, A., Tchouankoué, J. P., & Heilmeier, H. (2009). Soil and plant composition in the Noun river catchment basin, Western Cameroon: A contribution to the development of a biogeochemical baseline. *Environmental Geology*, *56*(7), 1427–1436. https://doi.org/10.1007/s00254-008-1237-9

Nriagu, J. O. (1989). A global assessment of natural sources of atmospheric trace metals. *Nature*, *338*(6210), 47–49. https://doi.org/10.1038/338047a0

Nyanganyura, D., Maenhaut, W., Mathuthu, M., Makarau, A., & Meixner, F. X. (2007). The chemical composition of tropospheric aerosols and their contributing sources to a continental background site in northern Zimbabwe from 1994 to 2000. *Atmospheric Environment*, *41*(12), 2644–2659. https://doi.org/10.1016/j.atmosenv.2006.11.015

Nygard, T., Steinnes, E., & Royset, O. (2012). Distribution of 32 elements in organic surface soils: Contributions from atmospheric transport of pollutants and natural sources. *Water, Air, & Soil Pollution*, *223*(2), 699–713. https://doi.org/10.1007/s11270-011-0895-5

O'Dowd, C. D., & de Leeuw, G. (2007). Marine aerosol production: A review of the current knowledge. *Philosophical Transactions of the Royal Society A*, *365*(1856), 1753–1774. https://doi.org/10.1098/rsta.2007.2043

Okin, G. S., Mahowald, N., Chadwick, O. A., & Artaxo, P. (2004). Impact of desert dust on the biogeochemistry of phosphorus in terrestrial ecosystems. *Global Biogeochemical Cycles*, *18*(2), GB2005. https://doi.org/10.1029/2003GB002145

Pacyna, J. M., & Pacyna, E. G. (2001). An assessment of global and regional emissions of trace metals to the atmosphere from anthropogenic sources worldwide. *Environmental Reviews*, *9*(4), 269–298. https://doi.org/10.1139/a01-012

Papadopoulos, F., Prochaska, C., Papadopoulos, A., Eskridge, K., & Kalavrouziotis, I. (2009). Mn and Zn micronutrients concentrations in acidic soils and source identification using multivariate statistical methods. *Communications in Soil Science and Plant Analysis*, *40*(15–16), 2357–2371. https://doi.org/10.1080/00103620903111285

Papastergios, G., Filippidis, A., Fernandez-Turiel, J.-L., Gimeno, D., & Sikalidis, C. (2011). Surface soil geochemistry for environmental assessment in Kavala Area, Northern Greece. *Water, Air, & Soil Pollution*, *216*(1–4), 141–152. https://doi.org/10.1007/s11270-010-0522-x

Parekh, P. P. (1990). A study of manganese from anthropogenic emissions at a rural site in the eastern United States. *Atmospheric Environment. Part A. General Topics*, *24*(2), 415–421. https://doi.org/10.1016/0960-1686(90)90122-4

Patel, K. S., Chikhlekar, S., Ramteke, S., Sahu, B. L., Dahariya, N. S., & Sharma, R. (2015). Micronutrient status in soil of Central India. *American Journal of Plant Sciences*, *06*(19), 3025–3037. https://doi.org/10.4236/ajps.2015.619297

Paye, H. D. S., de Mello, J. W., Pereira Abrahao, W. A., Fernandes Filho, E. I., Pinto Dias, L. C., Oliveira Castro, M. L., et al. (2010). Reference quality values for heavy metals in soils from Espirito Santo State, Brazil. *Revista Brasileira de Ciência do Solo*, *34*(6), 2041–2051. https://doi.org/10.1590/s0100-06832010000600028

Perez, N., Pey, J., Querol, X., Alastuey, A., Lopez, J. M., & Viana, M. (2008). Partitioning of major and trace components in PM_{10}-$PM_{2.5}$-PM_1 at an urban site in Southern Europe. *Atmospheric Environment*, *42*(8), 1677–1691. https://doi.org/10.1016/j.atmosenv.2007.11.034

Petroff, A., & Zhang, L. (2010). Development and validation of a size-resolved particle dry deposition scheme for application in aerosol transport models. *Geoscientific Model Development*, *3*(2), 753–769. https://doi.org/10.5194/gmd-3-753-2010

Phillips, C. A., Rogers, B. M., Elder, M., Cooperdock, S., Moubarak, M., Randerson, J. T., & Frumhoff, P. C. (2022). Escalating carbon emissions from North American boreal forest wildfires and the climate mitigation potential of fire management. *Science Advances*, *8*(17), eabl7161. https://doi.org/10.1126/sciadv.abl7161

Poggio, L., de Sousa, L. M., Batjes, N. H., Heuvelink, G. B. M., Kempen, B., Ribeiro, E., & Rossiter, D. (2021). SoilGrids 2.0: Producing soil information for the globe with quantified spatial uncertainty. *SOIL*, *7*(1), 217–240. https://doi.org/10.5194/soil-7-217-2021

Preda, M., & Cox, M. E. (2002). Trace metal occurrence and distribution in sediments and mangroves, Pumicestone region, southeast Queensland, Australia. *Environmental International*, *28*(5), 433–449. https://doi.org/10.1016/S0160-4120(02)00074-0

Prospero, J. M., Barrett, K., Church, T., Dentener, F., Duce, R. A., Galloway, J. N., et al. (1996). Atmospheric deposition of nutrients to the North Atlantic Basin. *Biogeochemistry*, *35*(1), 27–73. https://doi.org/10.1007/BF02179824

Puchelt, H., Kramar, U., Cumming, G. L., Krstic, D., Nöltner, T., Schöttle, M., & Schweikle, V. (1993). Anthropogenic Pb contamination of soils, southwest Germany. *Applied Geochemistry*, *8*, 71–73. https://doi.org/10.1016/S0883-2927(09)80014-0

Putaud, J. P., Raes, F., Van Dingenen, R., Brüggemann, E., Facchini, M. C., Decesari, S., et al. (2004). A European aerosol phenomenology - 2: Chemical characteristics of particulate matter at kerbside, urban, rural and background sites in Europe. *Atmospheric Environment*, *38*(16), 2579–2595. https://doi.org/10.1016/j.atmosenv.2004.01.041

Putaud, J. P., Van Dingenen, R., Alastuey, A., Bauer, H., Birmili, W., Cyrys, J., et al. (2010). A European aerosol phenomenology - 3: Physical and chemical characteristics of particulate matter from 60 rural, urban, and kerbside sites across Europe. *Atmospheric Environment*, *44*(10), 1308–1320. https://doi.org/10.1016/j.atmosenv.2009.12.011

Querol, X., Fernández-Turiel, J., & López-Soler, A. (1995). Trace elements in coal and their behaviour during combustion in a large power station. *Fuel*, *74*(3), 331–343. https://doi.org/10.1016/0016-2361(95)93464-O

Rashed, M. N. (2010). Monitoring of contaminated toxic and heavy metals, from mine tailings through age accumulation, in soil and some wild plants at Southeast Egypt. *Journal of Hazardous Materials*, *178*(1–3), 739–746. https://doi.org/10.1016/j.jhazmat.2010.01.147

Rathod, S. D., Hamilton, D. S., Mahowald, N. M., Klimont, Z., Corbett, J. J., & Bond, T. C. (2020). A mineralogy-based anthropogenic combustion-iron emission inventory. *Journal of Geophysical Research: Atmospheres*, *125*(17), e2019JD032114. https://doi.org/10.1029/2019JD032114

Rauch, J. N., & Pacyna, J. M. (2009). Earth's global Ag, Al, Cr, Cu, Fe, Ni, Pb, and Zn cycles. *Global Biogeochemical Cycles*, *23*(2), GB2001. https://doi.org/10.1029/2008GB003376

Rekasi, M., & Filep, T. (2012). Fractions and background concentrations of potentially toxic elements in Hungarian surface soils. *Environmental Monitoring and Assessment*, *184*(12), 7461–7471. https://doi.org/10.1007/s10661-011-2513-9

Richards, J. R., Schroder, J. L., Zhang, H., Basta, N. T., Wang, Y., & Payton, M. E. (2012). Trace elements in benchmark soils of Oklahoma. *Soil Science Society of America Journal*, *76*(6), 2031–2040. https://doi.org/10.2136/sssaj2012.0100

Ridley, D. A., Heald, C. L., & Ford, B. (2012). North African dust export and deposition: A satellite and model perspective. *Journal of Geophysical Research*, *117*(2), D02202. https://doi.org/10.1029/2011JD016794

Ridley, D. A., Heald, C. L., Kok, J. F., & Zhao, C. (2016). An observationally constrained estimate of global dust aerosol optical depth. *Atmospheric Chemistry and Physics*, *16*(23), 15097–15117. https://doi.org/10.5194/acp-16-15097-2016

Roca, N., Susana Pazos, M., & Bech, J. (2012). Background levels of potentially toxic elements in soils: A case study in Catamarca (a semiarid region in Argentina). *Catena*, *92*, 55–66. https://doi.org/10.1016/j.catena.2011.11.009

Roca-Perez, L., Boluda, R., & Perez-Bermudez, P. (2004). Soil-plant relationships, micronutrient contents, and cardenolide production in natural populations of Digitalis obscura. *Journal of Plant Nutrition and Soil Science*, *167*(1), 79–84. https://doi.org/10.1002/jpln.200320336

Roca-Perez, L., Gil, C., Cervera, M. L., Gonzalvez, A., Ramos-Miras, J., Pons, V., et al. (2010). Selenium and heavy metals content in some Mediterranean soils. *Journal of Geochemical Exploration*, *107*(2, SI), 110–116. https://doi.org/10.1016/j.gexplo.2010.08.004

Rodríguez, S., Alastuey, A., Alonso-Pérez, S., Querol, X., Cuevas, E., Abreu-Afonso, J., et al. (2011). Transport of desert dust mixed with North African industrial pollutants in the subtropical Saharan Air Layer. *Atmospheric Chemistry and Physics*, *11*(13), 6663–6685. https://doi.org/10.5194/acp-11-6663-2011

Rodríguez, S., Calzolai, G., Chiari, M., Nava, S., García, M. I., López-Solano, J., et al. (2020). Rapid changes of dust geochemistry in the Saharan Air Layer linked to sources and meteorology. *Atmospheric Environment*, *223*, 117186. https://doi.org/10.1016/j.atmosenv.2019.117186

Rodríguez, S., Cuevas, E., Prospero, J. M., Alastuey, A., Querol, X., López-Solano, J., et al. (2015). Modulation of Saharan dust export by the North African dipole. *Atmospheric Chemistry and Physics*, *15*(13), 7471–7486. https://doi.org/10.5194/acp-15-7471-2015

Rosswall, T. (1976). The internal nitrogen cycle between microorganisms, vegetation and soil. *Ecological Bulletins*, *22*, 157–167. Retrieved from http://www.jstor.org/stable/20112525

Rudnick, R. L., & Gao, S. (2003). The composition of the continental crust. In H. D. Holland & K. K. Turekian (Eds.), *Treatise on geochemistry, Vol. 3, The crust* (pp. 1–64). Elsevier-Pergamon. https://doi.org/10.1016/b0-08-043751-6/03016-4

Rusjan, D., Strlic, M., Pucko, D., Selih, V. S., & Korosec-Koruza, Z. (2006). Vineyard soil characteristics related to content of transition metals in a sub-Mediterranean winegrowing region of Slovenia. *Geoderma*, *136*(3–4), 930–936. https://doi.org/10.1016/j.geoderma.2006.06.014

Ryder, C. L., Highwood, E. J., Walser, A., Seibert, P., Philipp, A., & Weinzierl, B. (2019). Coarse and giant particles are ubiquitous in Saharan dust export regions and are radiatively significant over the Sahara. *Atmospheric Chemistry and Physics*, *19*(24), 15353–15376. https://doi.org/10.5194/acp-19-15353-2019

Saglam, C. (2017). Heavy metal concentrations in serpentine soils and plants from Kizildag National Park (Isparta) in Turkey. *Fresenius Environmental Bulletin*, *26*(6), 3995–4003.

Sako, A., Mills, A. J., & Roychoudhury, A. N. (2009). Rare earth and trace element geochemistry of termite mounds in central and northeastern Namibia: Mechanisms for micro-nutrient accumulation. *Geoderma*, *153*(1–2), 217–230. https://doi.org/10.1016/j.geoderma.2009.08.011

Salma, I., Maenhaut, W., Annegarn, H. J., Andreae, M. O., Meixner, F. X., & Garstang, M. (1997). Combined application of INAA and PIXE for studying the regional aerosol composition in southern Africa. *Journal of Radioanalytical and Nuclear Chemistry*, *216*(1), 143–148. https://doi.org/10.1007/BF02034512

Salonen, V.-P., & Korkka-Niemi, K. (2007). Influence of parent sediments on the concentration of heavy metals in urban and suburban soils in Turku, Finland. *Applied Geochemistry*, *22*(5), 906–918. https://doi.org/10.1016/j.apgeochem.2007.02.003

Sansone, F. J., Benitez-Nelson, C. R., Resing, J. A., DeCarlo, E. H., Vink, S. M., Heath, J. A., & Huebert, B. J. (2002). Geochemistry of atmospheric aerosols generated from lava-seawater interactions. *Geophysical Research Letters*, *29*(9), 1335. https://doi.org/10.1029/2001GL013882

Savoie, D. L., Prospero, J. M., Larsen, R. J., Huang, R., Izaguirre, M. A., Huang, T., et al. (1993). Nitrogen and sulfur species in Antarctic aerosols at Mawson, Palmer Station, and Marsh (King George Island). *Journal of Atmospheric Chemistry*, *17*(2), 95–122. https://doi.org/10.1007/BF00702821

Scanza, R. A., Mahowald, N., Ghan, S., Zender, C. S., Kok, J. F., Liu, X., et al. (2015). Modeling dust as component minerals in the Community Atmosphere Model: Development of framework and impact on radiative forcing. *Atmospheric Chemistry and Physics*, *15*(1), 537–561. https://doi.org/10.5194/acp-15-537-2015

Schlesinger, W. H., Klein, E. M., & Vengosh, A. (2017). Global biogeochemical cycle of vanadium. *Proceedings of the National Academy of Sciences of the United States of America*, *114*(52), E11092–E11100. https://doi.org/10.1073/pnas.1715500114

Schmidl, C., Marr, I. L., Caseiro, A., Kotianová, P., Berner, A., Bauer, H., et al. (2008). Chemical characterisation of fine particle emissions from wood stove combustion of common woods growing in mid-European Alpine regions. *Atmospheric Environment*, *42*(1), 126–141. https://doi.org/10.1016/j.atmosenv.2007.09.028

Schutgens, N. A. J., Gryspeerdt, E., Weigum, N., Tsyro, S., Goto, D., Schulz, M., & Stier, P. (2016). Will a perfect model agree with perfect observations? The impact of spatial sampling. *Atmospheric Chemistry and Physics*, *16*(10), 6335–6353. https://doi.org/10.5194/acp-16-6335-2016

Sedwick, P. N., Sholkovitz, E. R., & Church, T. M. (2007). Impact of anthropogenic combustion emissions on the fractional solubility of aerosol iron: Evidence from the Sargasso Sea. *Geochemistry, Geophysics, Geosystems*, *8*(10), Q10-Q06. https://doi.org/10.1029/2007GC001586

Selin, N. E. (2009). Global biogeochemical cycling of mercury: A review. *Annual Review of Environment and Resources*, *34*(1), 43–63. https://doi.org/10.1146/annurev.environ.051308.084314

Sen, I. S., & Peucker-Ehrenbrink, B. (2012). Anthropogenic disturbance of element cycles at the Earth's surface. *Environmental Science & Technology*, *46*(16), 8601–8609. https://doi.org/10.1021/es301261x

Sheikh-Abdullah, S. M. (2019). Availability of Fe, Zn, Cu, and Mn in soils of Sulaimani Governorate, Kurdistan Region, Iraq. *Soil Science*, *184*(3), 87–94. https://doi.org/10.1097/SS.0000000000000255

Sheppard, S. C., Grant, C. A., & Drury, C. F. (2009). Trace elements in Ontario soils - Mobility, concentration profiles, and evidence of non-point-source pollution. *Canadian Journal of Soil Science*, *89*(4), 489–499. https://doi.org/10.4141/cjss08033

Sierra, C. A., Trumbore, S. E., Davidson, E. A., Vicca, S., & Janssens, I. (2015). Sensitivity of decomposition rates of soil organic matter with respect to simultaneous changes in temperature and moisture. *Journal of Advances in Modeling Earth Systems*, *7*(1), 335–356. https://doi.org/10.1002/2014MS000358

Skordas, K., Papastergios, G., & Filippidis, A. (2013). Major and trace element contents in apples from a cultivated area of central Greece. *Environmental Monitoring and Assessment*, *185*(10), 8465–8471. https://doi.org/10.1007/s10661-013-3188-1

Smeltzer, G. G., Langille, W. M., & MacLean, K. S. (1962). Effects of some trace elements on grass and legume production in Nova Scotia. *Canadian Journal of Plant Science*, *42*(1), 46–52. https://doi.org/10.4141/cjps62-006

Smichowski, P., Gómez, D. R., Dawidowski, L. E., Giné, M. F., Bellato, A. C., & Reich, S. L. (2004). Monitoring trace metals in urban aerosols from Buenos Aires city. Determination by plasma-based techniques. *Journal of Environmental Monitoring*, *6*(4), 286–294. https://doi.org/10.1039/b312446k

Smith, D. B., Cannon, W. F., Woodruff, L. G., Solano, F., Kilburn, J. E., & Fey, D. L. (2013). Geochemical and mineralogical data for soils of the conterminous United States. U.S. Geological Survey Data Series 801 (p. 19). Retrieved from https://pubs.usgs.gov/ds/801/

Smith, R. D., Campbell, J. A., & Nielson, K. K. (1979). Characterization and formation of submicron particles in coal-fired plants. *Atmospheric Environment (1967)*, *13*(5), 607–617. https://doi.org/10.1016/0004-6981(79)90189-6

Spiro, P. A., Jacob, D. J., & Logan, J. A. (1992). Global inventory of sulfur emissions with 1° × 1° resolution. *Journal of Geophysical Research*, *97*(D5), 6023–6036. https://doi.org/10.1029/91JD03139

Stajković-Srbinović, O., Buntić, A., Rasulić, N., Kuzmanović, Đ., Dinić, Z., Delić, D., & Mrvić, V. (2018). Microorganisms in soils with elevated heavy metal concentrations in southern Serbia. *Archives of Biological Sciences*, *70*(4), 707–716. https://doi.org/10.2298/abs180504034s

Stankovic, D., Krstic, B., Knezevic, M., Sijacic-Nikolic, M., & Bjelanovic, I. (2012). Concentrations of heavy metals in soil in the area of the protected natural resource "Avala" in Belgrade. *Fresenius Environmental Bulletin*, *21*(2A), 495–502.

Steenari, B. M., Schelander, S., & Lindqvist, O. (1999). Chemical and leaching characteristics of ash from combustion of coal, peat and wood in a 12MW CFB – A comparative study. *Fuel*, *78*(2), 249–258. https://doi.org/10.1016/S0016-2361(98)00137-9

Stegemann, J. A., Roy, A., Caldwell, R. J., Schilling, P. J., & Tittsworth, R. (2000). Understanding environmental leachability of electric arc furnace dust. *Journal of Environmental Engineering*, *126*(2), 112–120. https://doi.org/10.1061/(ASCE)0733-9372(2000)126:2(112)

Stehouwer, R. C., Hindman, J. M., & MacDonald, K. E. (2010). Nutrient and trace element dynamics in blended topsoils containing spent foundry sand and compost. *Journal of Environmental Quality*, *39*(2), 587–595. https://doi.org/10.2134/jeq2009.0172

Steinnes, E., Lukina, N., Nikonov, V., Aamlid, D., & Røyset, O. (2000). A gradient study of 34 elements in the vicinity of a copper-nickel smelter in the Kola Peninsula. *Environmental Monitoring and Assessment*, *60*(1), 71–88. https://doi.org/10.1023/A:1006165031985

Stendahl, J., Berg, B., & Lindahl, B. D. (2017). Manganese availability is negatively associated with carbon storage in northern coniferous forest humus layers. *Scientific Reports*, *7*(1), 15487. https://doi.org/10.1038/s41598-017-15801-y

Sterckeman, T., Douay, F., Baize, D., Fourrier, H., Proix, N., & Schwartz, C. (2006a). Trace elements in soils developed in sedimentary materials from Northern France. *Geoderma*, *136*(3–4), 912–929. https://doi.org/10.1016/j.geoderma.2006.06.010

Sterckeman, T., Douay, F., Baize, D., Fourrier, H., Proix, N., Schwartz, C., & Carignan, J. (2006b). Trace element distributions in soils developed in loess deposits from northern France. *European Journal of Soil Science*, *57*(3), 392–410. https://doi.org/10.1111/j.1365-2389.2005.00750.x

Su, Y., & Yang, R. (2008). Background concentrations of elements in surface soils and their changes as affected by agriculture use in the desert-oasis ecotone in the middle of Heihe River Basin, North-west China. *Journal of Geochemical Exploration*, *98*(3), 57–64. https://doi.org/10.1016/j.gexplo.2007.12.001

Swap, R. J., Annegarn, H. J., Suttles, J. T., Haywood, J., Helmlinger, M. C., Hely, C., et al. (2002). The Southern African Regional Science Initiative (SAFARI 2000): Overview of the dry season field campaign. *South African Journal of Science*, *98*(3–4), 125–130.

Trum, F., Titeux, H., Ponette, Q., & Berg, B. (2015). Influence of manganese on decomposition of common beech (*Fagus sylvatica* L.) leaf litter during field incubation. *Biogeochemistry*, *125*(3), 349–358. https://doi.org/10.1007/s10533-015-0129-9

Tsai, S.-L., & Tsai, M.-S. (1998). A study of the extraction of vanadium and nickel in oil-fired fly ash. *Resources, Conservation and Recycling*, *22*(3–4), 163–176. https://doi.org/10.1016/S0921-3449(98)00007-X

Tsikritzis, L. I., Ganatsios, S. S., Duliu, O. G., Kavouridis, C. V., & Sawidis, T. D. (2002). Trace elements distribution in soil in areas of lignite power plants of Western Macedonia. *Journal of Trace and Microprobe Techniques*, *20*(2), 269–282. https://doi.org/10.1081/TMA-120003729

Tume, P., Bech, J., Reverter, F., Bech, J., Longan, L., Tume, L., & Sepúlveda, B. (2011). Concentration and distribution of twelve metals in Central Catalonia surface soils. *Journal of Geochemical Exploration*, *109*(1), 92–103. https://doi.org/10.1016/j.gexplo.2010.10.013

Tyler, G. (2004). Vertical distribution of major, minor, and rare elements in a Haplic Podzol. *Geoderma*, *119*(3–4), 277–290. https://doi.org/10.1016/j.geoderma.2003.08.005

UK Department for Environment, Food, and Rural Affairs (DEFRA). (n.d.). AURN network. Retrieved from https://uk-air.defra.gov.uk/data/

U.S. Geological Survey. (2022). Mineral commodity summaries 2022. https://doi.org/10.3133/mcs2022

van Diepen, L. T. A., Frey, S. D., Sthultz, C. M., Morrison, E. W., Minocha, R., Pringle, A., & Peters, D. P. C. (2015). Changes in litter quality caused by simulated nitrogen deposition reinforce the N-induced suppression of litter decay. *Ecosphere*, *6*(10), 205. https://doi.org/10.1890/ES15-00262.1

van Marle, M. J. E., Kloster, S., Magi, B. I., Marlon, J. R., Daniau, A.-L., Field, R. D., et al. (2017). Historic global biomass burning emissions for CMIP6 (BB4CMIP) based on merging satellite observations with proxies and fire models (1750–2015). *Geoscientific Model Development*, *10*(9), 3329–3357. https://doi.org/10.5194/gmd-10-3329-2017

van der Werf, G. R., Randerson, J. T., Collatz, G. J., Giglio, L., Kasibhatla, P. S., Arellano, A. F., Jr., et al. (2004). Continental-scale partitioning of fire emissions during the 1997 to 2001 El Niño/La Niña period. *Science*, *303*(5654), 73–76. https://doi.org/10.1126/science.1090753

Vance, N. C., & Entry, J. A. (2000). Soil properties important to the restoration of a Shasta red fir barrens in the Siskiyou Mountains. *Forest Ecology and Management*, *138*(1–3), 427–434. https://doi.org/10.1016/S0378-1127(00)00428-X

Vandenbussche, S., Callewaert, S., Schepanski, K., & DeMazière, M. (2020). North African mineral dust sources: New insights from a combined analysis based on 3D dust aerosol distributions, surface winds and ancillary soil parameters. *Atmospheric Chemistry and Physics*, *20*(23), 15127–15146. https://doi.org/10.5194/acp-20-15127-2020

Vanderzalm, J. L., Hooper, M. A., Ryan, B., Maenhaut, W., Martin, P., Rayment, P. R., & Hooper, B. M. (2003). Impact of seasonal biomass burning on air quality in the 'Top End' of regional Northern Australia. *Clean Air and Environmental Quality*, *37*(3), 28–34.

Vejnovic, J., Djuric, B., Lombnæs, P., & Singh, B. R. (2018). Concentration of trace and major elements in natural grasslands of Bosnia and Herzegovina in relation to soil properties and plant species. *Acta Agriculturae Scandinavica, Section B — Soil & Plant Science*, *68*(3), 243–254. https://doi.org/10.1080/09064710.2017.1388439

Virkkula, A., Aurela, M., Hillamo, R., Mäkelä, T., Pakkanen, T., Kerminen, V. M., et al. (1999). Chemical composition of atmospheric aerosol in the European subarctic: Contribution of the Kola Peninsula smelter areas, central Europe, and the Arctic Ocean. *Journal of Geophysical Research*, *104*(D19), 23681–23696. https://doi.org/10.1029/1999JD900426

Voutsa, D., & Samara, C. (2002). Labile and bioaccessible fractions of heavy metals in the airborne particulate matter from urban and industrial areas. *Atmospheric Environment*, *36*(22), 3583–3590. https://doi.org/10.1016/s1352-2310(02)00282-0

Wang, Z., Wade, A. M., Richter, D. D., Stapleton, H. M., Kaste, J. M., & Vengosh, A. (2022). Legacy of anthropogenic lead in urban soils: Co-occurrence with metal(loids) and fallout radionuclides, isotopic fingerprinting, and in vitro bioaccessibility. *Science of the Total Environment*, *806*, 151276. https://doi.org/10.1016/j.scitotenv.2021.151276

Watson, J. G., Chow, J. C., & Houck, J. E. (2001). $PM_{2.5}$ chemical source profiles for vehicle exhaust, vegetative burning, geological material, and coal burning in Northwestern Colorado during 1995. *Chemosphere*, *43*(8), 1141–1151. https://doi.org/10.1016/S0045-6535(00)00171-5

Webb, N. P., & Pierre, C. (2018). Quantifying anthropogenic dust emissions. *Earth's Future*, *6*(2), 286–295. https://doi.org/10.1002/2017EF000766

Wen, B., Li, L., Duan, Y., Zhang, Y., Shen, J., Xia, M., et al. (2018). Zn, Ni, Mn, Cr, Pb and Cu in soil-tea ecosystem: The concentrations, spatial relationship and potential control. *Chemosphere*, *204*, 92–100. https://doi.org/10.1016/j.chemosphere.2018.04.026

Whalen, E. D., Smith, R. G., Grandy, A. S., & Frey, S. D. (2018). Manganese limitation as a mechanism for reduced decomposition in soils under atmospheric nitrogen deposition. *Soil Biology and Biochemistry*, *127*, 252–263. https://doi.org/10.1016/j.soilbio.2018.09.025

Wiedinmyer, C., Lihavainen, H., Mahowald, N., Alastuey, A., Albani, S., Artaxo, P., et al. (2018). COARSEMAP: Synthesis of observations and models for coarse-mode aerosols. In *AGU fall meeting New Orleans, 2017*.

Wilcke, W., Krauss, M., & Kobza, J. (2005). Concentrations and forms of heavy metals in Slovak soils. *Journal of Plant Nutrition and Soil Science*, *168*(5), 676–686. https://doi.org/10.1002/jpln.200521811

Wong, M. Y., Rathod, S. D., Marino, R., Li, L., Howarth, R. W., Alastuey, A., et al. (2021). Anthropogenic perturbations to the atmospheric molybdenum cycle. *Global Biogeochemical Cycles*, *35*(2), e2020GB006787. https://doi.org/10.1029/2020GB006787

Woo, D. K., & Seo, Y. (2022). Effects of elevated temperature and abnormal precipitation on soil carbon and nitrogen dynamics in a Pinus densiflora forest. *Frontiers in Forests and Global Change*, *5*, 1051210. https://doi.org/10.3389/ffgc.2022.1051210

Xianmo, Z., Yushan, L., Xianglin, P., & Shuguang, Z. (1983). Soils of the loess region in China. *Geoderma*, *29*(3), 237–255. https://doi.org/10.1016/0016-7061(83)90090-3

Xiao, Y. H., Liu, S. R., Tong, F. C., Kuang, Y. W., Chen, B. F., & Guo, Y. D. (2014). Characteristics and sources of metals in TSP and $PM_{2.5}$ in an urban Forest Park at Guangzhou. *Atmosphere*, *5*(4), 775–787. https://doi.org/10.3390/atmos5040775

Yalcin, M. G., Battaloglu, R., & Ilhan, S. (2007). Heavy metal sources in sultan marsh and its neighborhood, Kayseri, Turkey. *Environmental Geology*, *53*(2), 399–415. https://doi.org/10.1007/s00254-007-0655-4

Yang, C., Guo, R., Liu, R., Yue, Q., Ren, X., & Wu, Z. (2012). PCA analysis and concentration of heavy metal in the soil, Guangdong, China. *Advances in Environmental Science and Engineering*, *518–523*, 1952–1955. https://doi.org/10.4028/www.scientific.net/AMR.518-523.1952

Yang, S., Zhou, D., Yu, H., Wei, R., & Pan, B. (2013). Distribution and speciation of metals (Cu, Zn, Cd, and Pb) in agricultural and non-agricultural soils near a stream upriver from the Pearl River, China. *Environmental Pollution*, *177*, 64–70. https://doi.org/10.1016/j.envpol.2013.01.044

Yilmaz, F., Yilmaz, Y. Z., Ergin, M., Erkol, A. Y., Muftuoglu, A. E., & Karakelle, B. (2003). Heavy metal concentrations in surface soils of Izmit Gulf region, Turkey. *Journal of Trace and Microprobe Techniques*, *21*(3), 523–531. https://doi.org/10.1081/TMA-120023068

Yu, C., Cheng, J. J., Jones, L. G., Wang, Y. Y., Faillace, E., Loureiro, C., & Chia, Y. P. (1993). Data collection handbook to support modeling the impacts of radioactive material in soil. United States. https://doi.org/10.2172/10162250

Yu, C., Peng, B., Peltola, P., Tang, X., & Xie, S. (2012). Effect of weathering on abundance and release of potentially toxic elements in soils developed on Lower Cambrian black shales, P. R. China. *Environmental Geochemistry and Health*, *34*(3), 375–390. https://doi.org/10.1007/s10653-011-9398-y

Yu, H., Chin, M., Yuan, T., Bian, H., Remer, L. A., Prospero, J. M., et al. (2015). The fertilizing role of African dust in the Amazon rainforest: A first multiyear assessment based on data from cloud-aerosol lidar and infrared pathfinder satellite observations. *Geophysical Research Letters*, *42*(6), 1984–1991. https://doi.org/10.1002/2015GL063040

Zak, D. R., Freedman, Z. B., Upchurch, R. A., Steffens, M., & Kögel-Knabner, I. (2017). Anthropogenic N deposition increases soil organic matter accumulation without altering its biochemical composition. *Global Change Biology*, *23*(2), 933–944. https://doi.org/10.1111/gcb.13480

Zender, C. S., Bian, H., & Newman, D. (2003). Mineral Dust Entrainment and Deposition (DEAD) model: Description and 1990s dust climatology. *Journal of Geophysical Research*, *108*(D14), 4416. https://doi.org/10.1029/2002JD002775

Zhang, H., Wang, S., Hao, J., Wan, L., Jiang, J., Zhang, M., et al. (2012). Chemical and size characterization of particles emitted from the burning of coal and wood in rural households in Guizhou, China. *Atmospheric Environment*, *51*, 94–99. https://doi.org/10.1016/j.atmosenv.2012.01.042

Zhang, L., Zheng, Q., Liu, Y., Liu, S., Yu, D., Shi, X., et al. (2019). Combined effects of temperature and precipitation on soil organic carbon changes in the uplands of eastern China. *Geoderma*, *337*, 1105–1115. https://doi.org/10.1016/j.geoderma.2018.11.026

Zhang, X.-Y., Tang, L.-S., Zhang, G., & Wu, H.-D. (2009). Heavy metal contamination in a typical mining town of a minority and mountain area, South China. *Bulletin of Environmental Contamination and Toxicology*, *82*(1), 31–38. https://doi.org/10.1007/s00128-008-9569-4

Zhao, B., Zhuang, Q., Shurpali, N., Köster, K., Berninger, F., & Pumpanen, J. (2021). North American boreal forests are a large carbon source due to wildfires from 1986 to 2016. *Scientific Reports*, *11*(1), 7723. https://doi.org/10.1038/s41598-021-87343-3

Zhao, F., Wu, Y., Hui, J., Sivakumar, B., Meng, X., & Liu, S. (2021). Projected soil organic carbon loss in response to climate warming and soil water content in a loess watershed. *Carbon Balance and Management*, *16*(1), 24. https://doi.org/10.1186/s13021-021-00187-2

Zorer, Ö., Ceylan, H., & Doğru, M. (2009). Determination of heavy metals and comparison to gross radioactivity concentration in soil and sediment samples of the Bendimahi River Basin (Van, Turkey). *Water, Air, & Soil Pollution*, *196*(1–4), 75–87. https://doi.org/10.1007/s11270-008-9758-0

References From the Supporting Information

Batjes, N. H. (1997). A world data set of derived soil properties by FAO-UNESCO soil unit for global modelling. *Soil Use and Management*, *13*, 9–16.

Soil Survey Staff. (2011). Soil survey laboratory information manual soil survey investigations report No. 45.